Automation in Construction 147 (2023) 104714

Contents lists available at ScienceDirect

Automation in Construction

journal homepage: www.elsevier.com/locate/autcon

Automated detection of construction work at heights and deployment of safety hooks using IMU with a barometer

Hunsang Choo [a], Bogyeong Lee [b], Hyunsoo Kim [b], Byungjoo Choi [c,*]

[a] Department of Smart Convergence Architecture, Ajou University, 206 Worldcup-ro, Suwon-si 16499, Gyeonggi-do, Republic of Korea
[b] Department of Architectural Engineering, Dankook University, 152 Jukjeon-ro, SYongin-si 16890, Gyeonggi-do, Republic of Korea
[c] Department of Architectural Engineering, Ajou University, 206 Worldcup-ro, Suwon-si 16499, Gyeonggi-do, Republic of Korea

ARTICLE INFO

Keywords:
Fall from height
Wearable sensor
Machine learning
Safety management
Construction safety

ABSTRACT

An automated system that identifies work at height and the fastening state of safety hooks using wearable sensors was developed to prevent falls from height (FFH). This system estimates the altitudes of workers based on the atmospheric pressure measured by a barometer and acceleration and gyroscopic signals from an inertial measurement unit (IMU). The fastening state of the safety hooks of workers at height is determined with the data collected by the IMU sensor and machine learning algorithms. Although researchers have tried to detect unsafe work conditions and unsafe behaviors at height, the complicated tasks and dynamic work conditions have discouraged them from establishing precise methodologies for effective and timely detection. To validate the system of this study, on-site field experiments were conducted to collect data from 20 construction workers. The performance of the developed model was assessed with leave-one-subject-out cross-validation (LOSOCV) to accommodate a wide range of new workers and their working conditions. According to the results, the work-at-height identification system is 96% accurate, while the safety hook attachment detection system is 86% accurate. The findings of this study fill knowledge gaps by providing ways of identifying workers working at height and detecting the fastening state of safety hooks in a non-invasive and objective manner. The results are expected to improve safety management at construction sites by minimizing the FFH risk for workers working at height.

1. Introduction

Despite its continuous efforts to improve workplace safety, the construction industry still remains one of the most dangerous industries worldwide [1,2]. For instance, construction industry workers account for only 5% of all industrial workers in the US [3,4]; however, the proportion of work fatalities or fatal work injuries in the construction industry is 25% [5,104]. Approximately 36% of these fatal injuries are attributed to falls at height (FFH), which are one of the leading causes of fatalities in the construction industry [6]. Other countries, including Australia, China, and Korea, have also experienced enormous economic, productive, and human losses due to FFH [7,8].

According to theories concerning accident causation [9,10,11], safety incidents can be ascribed to the interaction among the unsafe behaviors of workers and unsafe working conditions. The Swiss cheese model [proposed by Reason [12]] demonstrates that accidents are subject to the interplay among unsafe conditions, unsafe behaviors, and other failures (e.g., organizational influences, unsafe supervision, preconditions for unsafe acts, and unsafe acts themselves). Working at height is an unsafe condition that can lead to FFH at construction sites; unsafe behavior represents the failure of workers at height to fasten their safety hook properly to an anchor point. Thus, to prevent FFH at construction sites, unsafe conditions (i.e., work at height) and unsafe behavior (i.e., improper fastening or unfastening of the safety hook to/from an anchor point) must be systematically controlled.

The Occupational Safety and Health Administration (OSHA) of the US imposes mandatory measures for preventing FFH during work above a certain height (i.e., 6 ft) [13]. A series of FFH prevention steps are taken at construction sites: safety training and education [14], safety nets or safety guardrail systems [15], and monitoring personal protective equipment (PPE) [16]. Although safety training and education represent a proactive strategy, they have limitations regarding the direct prevention of FFH [17]. In addition, safety nets are not preventive; they are follow-up measures for FFHs [15]. Although safety guardrail systems can prevent FFH, they are passive and cannot proactively protect workers from accidents caused by their unsafe behaviors. By contrast,

* Corresponding author.
E-mail addresses: chooson@ajou.ac.kr (H. Choo), bglee_@dankook.ac.kr (B. Lee), hkim13@dankook.ac.kr (H. Kim), bchoi@ajou.ac.kr (B. Choi).

https://doi.org/10.1016/j.autcon.2022.104714
Received 11 August 2022; Received in revised form 12 November 2022; Accepted 18 December 2022
Available online 28 December 2022
0926-5805/

PPE (e.g., a safety helmet, safety belt, and safety lanyard) is a useful proactive measure that significantly reduces the risk of fatalities and injuries. In particular, a properly fastened safety hook is crucial as it can proactively protect workers whenever the risk of FFH arises [18]. Nonetheless, many workers at construction sites find the safety hook system inconvenient and do not securely attach their safety hooks, which can lead to FFH [19,20,16]. Therefore, the unsafe conditions (i.e., work at height) and unsafe work behaviors (i.e., improper fastening or unfastening of the safety hook) must be closely and continuously monitored.

Safety managers at a construction site depend heavily on manual and visual monitoring to manage the behaviors of workers [21,22]. However, compared to those of other industries, the constant and dynamic changes in the tasks and working conditions at construction sites [23,24,25,26], limited number of safety managers, and time constraints make manual monitoring impossible [27]. To overcome these limitations, researchers have applied IT-based automated safety monitoring methods as an effective alternative [28,8,29,30]. There are two representative IT-based monitoring approaches: 1) sensor-based monitoring and 2) computer vision-based monitoring (Fang et al., 2018). The sensor-based approach enables the analysis of signals from the equipment, materials, and body movements and physiological state of individual workers at a construction site [31,32,33,15]. The computer vision-based approach facilitates the analysis of visual data (e.g., images and videos) to gather data on the locations, distances, and movements of objects at a construction site [34,35].

The sensor-based approach enables inspectors or managers to collect signals from physiological and physical movements of individual workers [33,36,105]. Thus, individual workers at a construction site where complicated and multiple tasks are simultaneously performed can be micro-managed [106]. Furthermore, the recent advancement in the field of wearable sensor technologies enables the continuous and non-invasive collection of data [37]. In this study, a wearable-sensor-based approach was used to collect data on the movements of individual workers in a non-invasive manner. We tried to prevent FFH resulting from improper fastening or unfastening of safety hooks with continuous and automated monitoring with wearable sensors. Based on the analysis of the atmospheric pressure with a barometer, workers working above a certain height can be accurately identified through the differences in the altitudes of the sensors [38,39]. Body movement signals collected by an inertial measurement unit (IMU) are of great value when the behaviors of individual workers are classified through machine learning algorithms [40,41,42,43,107]. In short, by estimating the altitudes of workers with a barometer, workers at height (i.e., under unsafe conditions) can automatically be identified. In addition, IMU sensor data and machine learning can be employed to monitor automatically improper fastening or unfastening actions of the safety hook (i.e., unsafe behaviors of workers at height).

Many researchers have addressed safety-related accidents at construction sites through automated monitoring of unsafe conditions and unsafe behaviors of workers, including the improper use of PPE. For example, Park et al. [44] developed an indoor positioning system (IPS) to identify workers working in unsafe areas that have been determined by a construction supervisor based on Internet of Things (IoT) sensors such as Bluetooth Low Energy. Liu et al. [38] combined the IPS, building information modeling, and cloud communication to develop a monitoring system that identifies workers who are approaching predefined fall hazard areas. Piao et al. [22] utilized computer vision and dynamic Bayesian networks to develop a fall risk assessment framework for construction workers.

These researchers have presented methods that identify and manage workers working in areas with fall hazards in a two-dimensional plane; they have rarely focused on identifying workers at height and had limited to detect their unsafe behavior (i.e., improper fastening or unfastening of safety hooks). Some researchers have concentrated on sensor- or computer vision-based automated monitoring systems to detect the improper use or non-use of PPE. Gomez-de-Gabriel et al. [20] explored the feasibility of detecting proper PPE use by detecting the safety belts of workers with IoT sensors. Moreover, Yang and Shami [45] used IoT sensors (e.g., optical pulse sensors, IMU sensors, force sensing resistors, and light-dependent resistors) to develop a pair check system for PPE (e.g., the hardhat, safety belt, safety glasses, safety gloves, and safety boots) and tools (e.g., hammers). However, the researchers have only checked whether the workers safely wore their safety belts and hardhats; thus, the identification of the fastening state of safety hooks is limited. Song et al. [101] employed an assumption pertaining to the safety hook fastening status: When the safety hook is securely attached to an anchor point, it moves considerably less than the workers do. Nevertheless, they focused only on identifying the status of the safety hook attachment and did not consider work-at-height. Fang et al. [17], Wang et al. [46], Wu et al. [47], and Xiong and Tang [48] developed computer vision-based monitoring systems to assess whether workers wear PPE properly. These systems also check whether the worker at height has properly attached the safety hook to an anchor point. To overcome the limitations of previously published studies, Khan et al. [49] and Khan et al. [13] used computer vision, IMU sensors, and barometers to develop monitoring systems for safety hooks. Unfortunately, their monitoring system, which is suitable for scaffolds, has limited applicability because it does not cover the diverse range of tasks performed at construction sites (e.g., working on horse and mobile scaffolds, ladders, and at ground level). Moreover, individual variations were not considered in the validation, which may have limited the generalizability of their results.

In this study, an automated monitoring system was developed to identify workers working at height (i.e., under unsafe conditions) for a wide range of construction tasks and improperly attached safety hooks (i.e., unsafe behavior) to prevent FFH proactively. Therefore, signals from a barometer and IMU sensors and a method for identifying work at height and the fastening state of safety hooks at height were applied. To verify the applicability of the developed system at actual construction sites, data were collected from individual workers working under different conditions at a construction site (i.e., work on mobile and horse scaffolds, ladders, and the ground level). The developed system consists of a base module installed on the floor of each story, a belt module, and a hook module worn by workers. A barometer sensor and IMU sensors are embedded in each module. The signals (e.g., the atmospheric pressure and acceleration and gyroscopic signals) from the barometer and IMU sensors on the base and belt modules are processed to estimate the altitudes of the sensors; thereby, workers working at height can be identified by calculating the differences in the altitudes. Based on the acceleration signals of the IMU sensors in the belt and hook modules, a machine learning model was developed to detect the fastening state of safety hooks of workers at height. We believe that this study will lay the foundation for an automated safety monitoring framework for workers at height that proactively prevents FFH and ultimately improves safety management in the construction industry. This study contributes to the methodological and practical advances as follows:

- The method proposed herein can accurately identify the workers working above a certain height based on an analysis of the ambient atmospheric pressure by using barometer data, which has rarely been attempted yet. The use of barometer data reduces the amount of calculations required because only the workers working at a height are screened to check whether their safety hooks are properly fastened.
- In this study, the status of the safety hook (i.e., whether it is properly fastened) is considered, which is more critical for proactive safety monitoring, unlike most of the previous studies that have focused on the existence of PPE.
- The applicability of the proposed method is improved by considering a more diverse range of tasks performed at construction sites (e.g., working on horse and mobile scaffolds, ladders, and at ground level).

- The method proposed herein considers variations in subject-specific characteristics while performing validation using the LOSOCV, which extends its generalizability to newly added workers.

The remainder of this paper is organized as follows: The following section details the field experiments conducted in different scenarios at an actual construction site. It presents the analysis of the data collected from the experiments and the development of the safety monitoring system for identifying workers at height and detecting the fastening state of safety hooks. Subsequently, the results are presented, followed by a discussion on the validity of the system in detecting the fastening state of safety hooks of workers at height based on the analytical results. Finally, the findings are summarized.

2. Methodology

This section explains how workers at height and improperly attached safety hooks can be detected with wearable sensors. Fig. 1 presents the research framework. First, a preliminary experiment was conducted to select the location for the installation of a wearable sensor for the accurate identification of workers at height. Three potential locations (i.e., the safety helmet, safety belt, and worker's ankle) were considered. The preliminary test results indicated that worker identification at height was the most accurate when the sensor module was attached to the back of the workers' safety belt rather than the helmet or the ankle. In addition, the back of the workers' safety belt was found to be a relevant location where the sensor was not in direct contact with the worker's body, resulting in reduced discomfort during work. Therefore, the sensor was attached to the back of the safety belt (i.e., the belt module), in accordance with the results of the experiment. To verify the system's applicability on site, field experiments were performed that simulate both work at height and a lower level (which is defined as work performed below the "work at height" threshold) that occur at actual construction sites; the data were collected from individual workers. Artifacts in the collected data were eliminated through data preprocessing. The cleaned data for work-at-height and improperly attached safety hooks are presented in Fig. 1(a) and (b), respectively. To identify work at height, the atmospheric pressure and acceleration and gyroscopic signals from the base and belt modules were recorded. These signals were fused with Kalman and complementary filters to estimate the altitude of each module (i.e., the base and belt module). The differences in the altitudes estimated with the base and belt modules were computed and analyzed with rule-based analysis to determine the work at height. To detect improperly attached safety hooks, acceleration signals were collected from the hook and belt modules; these signals were used to develop a machine learning classification model. When the safety hook is securely attached to an anchor point, it moves much less than the worker. By contrast, when the safety hook, which is usually attached to the safety belt, is not attached to an anchor point, it moves in a similar pattern as the worker. In other words, depending on the state of safety hooks, workers and their safety hooks move in similar or different patterns. This movement enabled us to utilize acceleration signals from the belt and hook modules and to train machine learning models to detect the state of safety hooks. Leave-one-subject-out cross-validation (LOSOCV), rather than the widely used cross-validation method, was used to evaluate the performance of the machine learning models for detecting the state of safety hooks for workers at height; thereby, the generalizability of the model to newly introduced workers was assessed in a more precise manner.

2.1. Collection of field data

Fig. 2 shows data collected from field experiments to identify workers at height and the fastening state of their safety hooks. The field experiments were conducted at an actual construction site; twenty subjects participated in the experiments. The tasks in the field

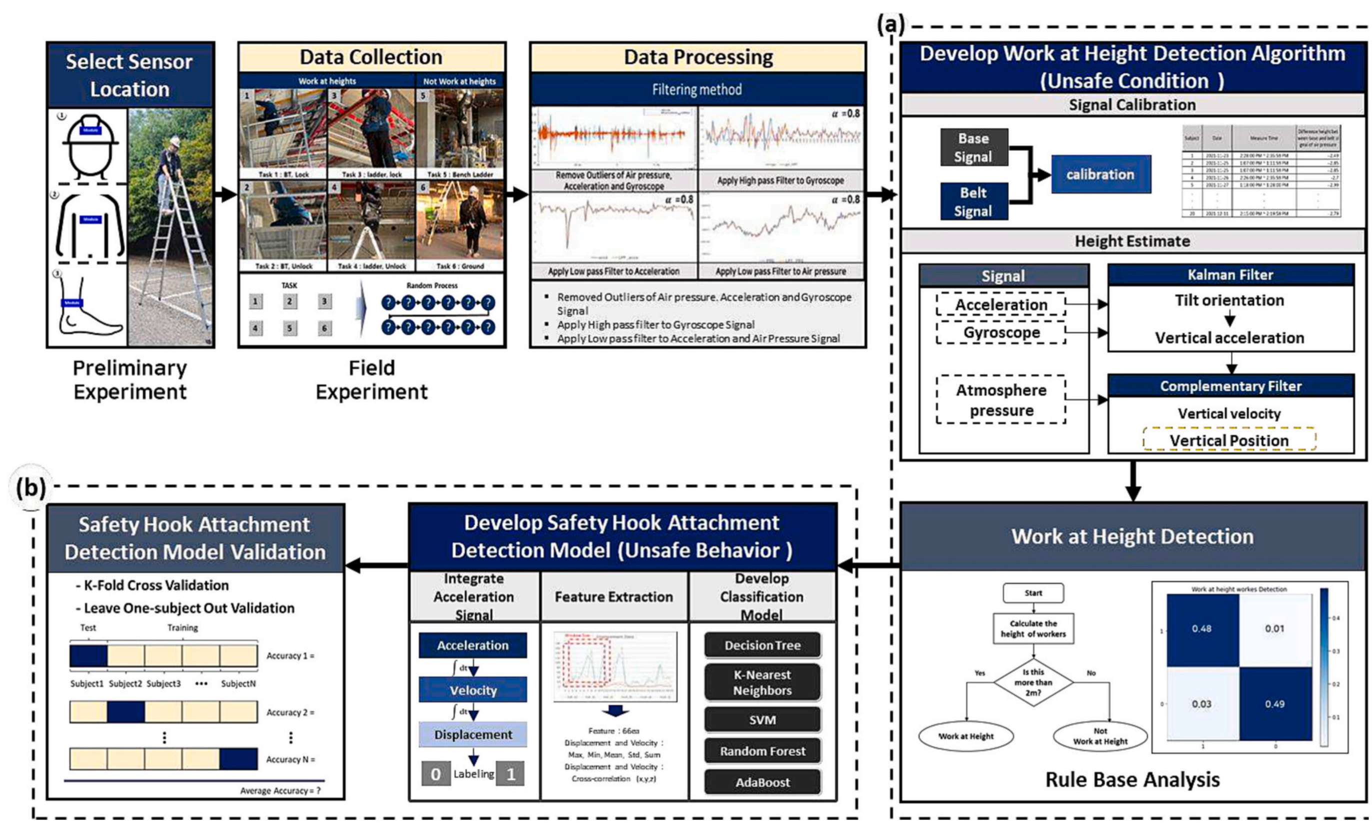

Fig. 1. Research framework.

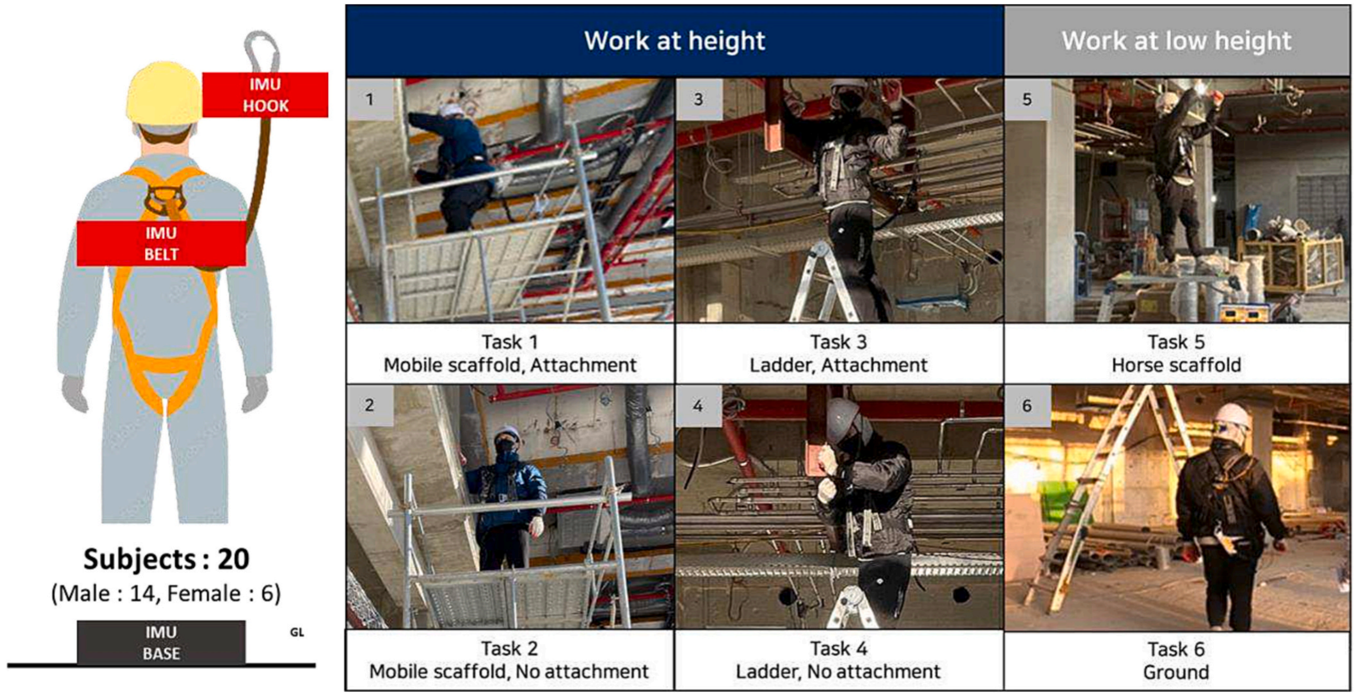

Fig. 2. Field experiment.

experiments involved typical work-at-height tasks and lower-level tasks based on interviews with on-site supervisors and field observations. Table 1 lists four work-at-height and two lower-level work types performed in the field experiment. Because mobile-scaffold and ladder tasks are performed above 2 m, they are classified as work at height according to the standards of OSHA (1995) [50] and Korea Occupational Safety and Health Agency (KOSHA) [51]; horse scaffold and ground tasks are classified as lower-level work. The subjects performed masonry work on mobile scaffolds that were more than 3 m high. During ladder tasks, the subjects installed plumbing in the ceiling at heights of more than 2 m. The mobile-scaffold and ladder tasks, which are classified as work at height, were further divided into two classes: the safety hook was securely attached and the safety hook was not attached. The experiments were designed to examine whether the model is capable of accurately distinguishing tasks that are classified as work at height from those that are not. For example, tasks performed on 3 m mobile scaffolds are clearly classified as work at height. However, tasks on ladders and horse scaffolds are performed at approximately 2 and 1.2 m, respectively, which are similar to the height standard (2 m) set by OSHA and KOSHA for work at height. Therefore, the experiments show the ability of the model to distinguish these tasks accurately. For tasks that involve horse scaffolds, the subjects simulated a typical job with interior finishes (e.g., painting and wallpapering) based on interviews with on-site supervisors and Jeong (2016). Finally, the subjects performed plain jobs and moved around workstations to simulate ground-level tasks. These six tasks were performed twice in twelve sections. The order of the tasks was randomized to avoid biases that may arise from a fixed experimental sequence. Each scenario took 3 min, and the experiments were conducted for three weeks (from November 23 to December 11, 2021).

Data were collected from the base, belt, and hook sensor modules. The base module was installed on a slab, whereas the belt and hook modules were attached to the back of the worker's safety belt and safety hook, respectively. Each module consists of a barometer and an IMU sensor. The atmospheric pressure signals from the barometer and the acceleration and gyroscopic signals from the IMU sensor were collected at 8 Hz. These signals were stored in a database server, pre-processed, and used to identify workers at height and the fastening state of their safety hooks. When identifying work at height, the base module serves as a reference point; the altitude difference between the base and belt modules indicates whether the corresponding task is performed at height. The acceleration signals from the IMU sensors on the belt and hook modules were employed to detect the safety hooks. The data that support the findings of this study are openly available in Mendely data [108].

Table 1
Summary of tasks for field experiments.

Task	Type of work	Work at height	Fastening state of safety hook	Height
Task 1	Mobile scaffold	Yes	Yes	>3 m
Task 2	Mobile scaffold	Yes	No	>3 m
Task 3	Ladder	Yes	Yes	>2 m
Task 4	Ladder	Yes	No	>2 m
Task 5	Horse scaffold	No	-	0.9–1.2 m
Task 6	Ground	No	-	0 m

2.2. Data pre-processing

The first step in data pre-processing was to remove outliers from the atmospheric pressure, acceleration, and gyroscopic signals. In the removal process, the median absolute deviation (MAD) method was used [53]. The "outlier" definition of Aroni et al. [54] was applied: the observed data points that exceed 3 MAD from the median were excluded. The outliers were substituted with previous values, as in the method used by Zhao et al. [55] (Fig. 3).

After the removal of outliers from each signal, customized filtering, which was tailored to the characteristics of each signal, was employed to remove artifacts. A low pass filter offers easy passage to low-frequency signals and rejects high-frequency signals, whereas a high pass filter does the opposite. Owing to the different frequency characteristics of sensor signals [56], the differences must be considered, and the two

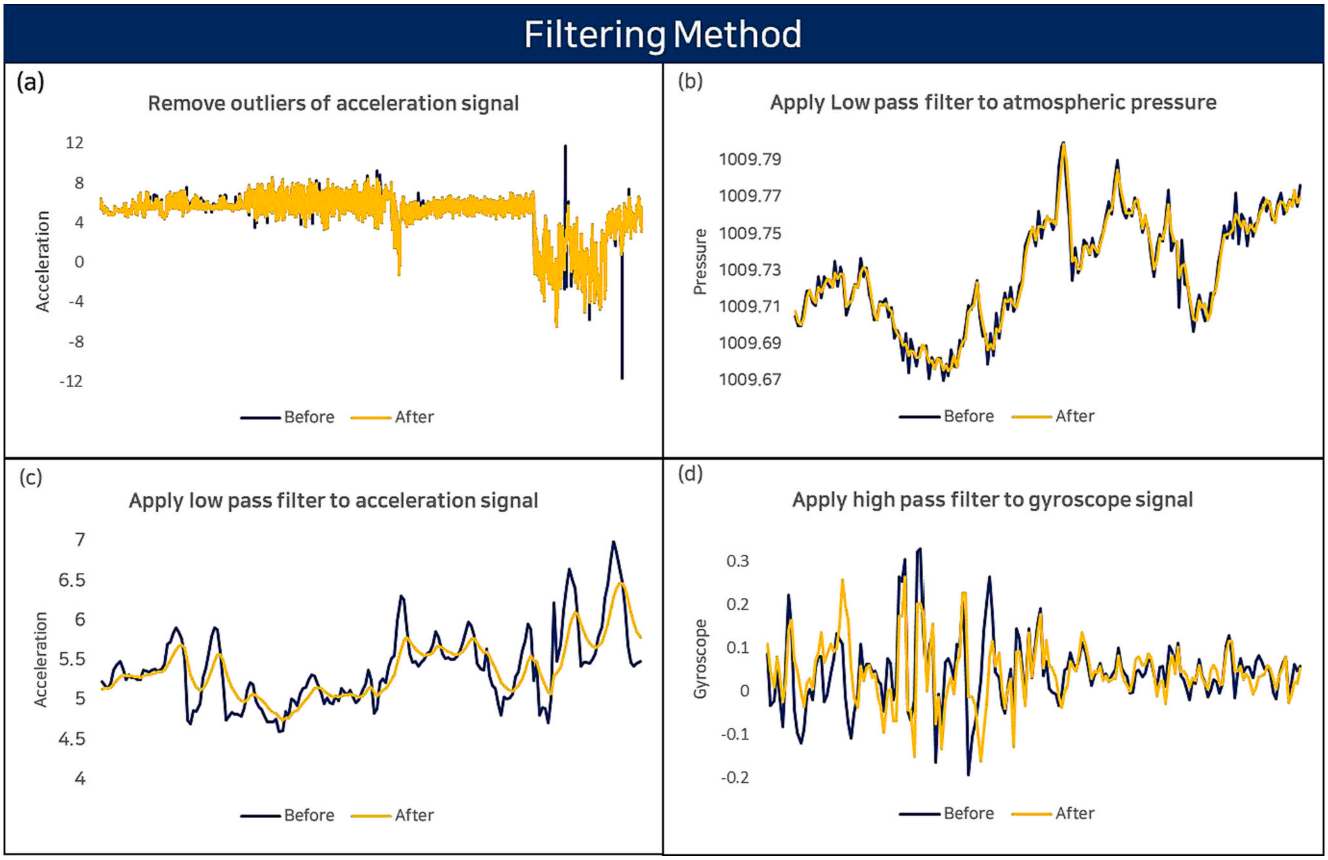

Fig. 3. Differences between unprocessed and pre-processed signals.

filters must aptly be used to remove noise. Atmospheric pressure and acceleration signals feature low frequencies; hence, the low pass filter does a better job of removing noise [56], whereas the high pass filter more effectively removes noise of gyroscopic signals (which have high frequencies) [56]. Eqs. (1) and (2) represent the low and high pass filters, respectively; the coefficient alpha (α) has a value between 0 and 1:

$$x_n = \alpha x_{n-1} + (\alpha - 1)x_n \tag{1}$$

$$y_n = \alpha y_{n-1} + \alpha(u_n - u_{n-1}), (y: \text{predicted value}, u: \text{input}) \tag{2}$$

2.3. Detection of work at height

All pre-processed signals from the base and belt modules were fused with Kalman and complementary filters and used to estimate the heights of workers. First, roll ϕ and pitch θ, which are the horizontal attitude angles, were estimated based on the acceleration signals. These horizontal attitude angles were fused with gyroscopic signals and Kalman filtering to estimate the final attitude angles, which were then used to predict the vertical acceleration from an inertial frame of reference. The signals collected from each acceleration sensor are represented as follows: $x_{acc} = [f_x\ f_y\ f_z]^T$. The attitude angles are $[roll \quad pitch \quad yaw]^T$, where ϕ and θ (i.e., the horizontal attitude angles)

are $\phi = tan^{-1}\left(\frac{f_y}{f_z}\right)$ and $\theta = tan^{-1}\left(\frac{f_x}{\sqrt{f_y^2+f_z^2}}\right)$; this results in the following equation:

$$x_{Attitude\_acc} = \left[\phi_{acc} = tan^{-1}\left(\frac{f_y}{f_z}\right), \quad \theta_{acc} = tan^{-1}\left(\frac{f_x}{\sqrt{f_y^2+f_z^2}}\right) \quad \psi_{acc}\right]^T \tag{3}$$

The value measured using the gyroscopic sensor $x_{gyr} = [p \quad q \quad r]^T$ can alternatively be expressed using the attitude angles $[\phi \quad \theta \quad \psi]^T$. The following equation describes the relationship among the gyroscopic signals and attitude angles:

$$\begin{pmatrix} \dot{\phi} \\ \dot{\theta} \\ \dot{\psi} \end{pmatrix} = \begin{bmatrix} 1 & sin\phi\ tan\theta & cos\phi\ tan\theta \\ 0 & cos\theta & -sin\phi \\ 0 & sin\phi/cos\theta & cos\phi/cos\theta \end{bmatrix} \begin{pmatrix} p \\ q \\ r \end{pmatrix} \tag{4}$$

The two attitude angles determined based on the acceleration and gyroscopic signals are mutually complementary and can be fused with the Kalman filter to estimate the final attitude angle in a more precise manner [57].

Finally, the Kalman filter algorithm calculates the estimated value $\hat{x}_k$ and error covariance P_k (when the measured z_k value is available); $\hat{x}_k$ is a physical variable and the final attitude angle in this case. The measured value z_k is for $x_{Attitude\_acc}$. Creating the Kalman filtering system model entails the following equation:

$$\hat{x}_{k+1} = A\hat{x}_k + w_k \Longleftrightarrow \begin{pmatrix} \dot{\phi} \\ \dot{\theta} \\ \dot{\psi} \end{pmatrix} = \begin{bmatrix} \bullet \end{bmatrix} \begin{pmatrix} \phi \\ \theta \\ \psi \end{pmatrix} \tag{5}$$

To implement the system model, the relationship between the quaternion and gyroscope $\hat{x}_k$ is converted:

$$\begin{Bmatrix} \dot{q}_1 \\ \dot{q}_2 \\ \dot{q}_3 \\ \dot{q}_4 \end{Bmatrix} = \frac{1}{2} \begin{bmatrix} 0 & -p & -q & -r \\ p & 0 & r & -q \\ q & -r & 0 & p \\ r & q & -p & 0 \end{bmatrix} \begin{Bmatrix} q_1 \\ q_2 \\ q_3 \\ q_4 \end{Bmatrix} \tag{6}$$

z_k can be represented with a column vector and $x_{Attitude\_acc}$:

$$z_k = \begin{bmatrix} cos\frac{\phi}{2}cos\frac{\theta}{2}cos\frac{\psi}{2} + sin\frac{\phi}{2}sin\frac{\theta}{2}sin\frac{\psi}{2} \\ sin\frac{\phi}{2}cos\frac{\theta}{2}cos\frac{\psi}{2} - cos\frac{\phi}{2}sin\frac{\theta}{2}sin\frac{\psi}{2} \\ cos\frac{\phi}{2}sin\frac{\theta}{2}cos\frac{\psi}{2} + sin\frac{\phi}{2}cos\frac{\theta}{2}sin\frac{\psi}{2} \\ cos\frac{\phi}{2}cos\frac{\theta}{2}sin\frac{\psi}{2} - sin\frac{\phi}{2}sin\frac{\theta}{2}cos\frac{\psi}{2} \end{bmatrix} \tag{7}$$

The matrix A, which has the form of a system model, indicates how the system behaves over time in implementing the Kalman filter. It can be expressed with the quaternions of Eq. (8) with gyroscopic signals:

$$A = \mathrm{I} + \frac{1}{2}dt \begin{bmatrix} 0 & -p & -q & -r \\ p & 0 & r & -q \\ q & -r & 0 & p \\ r & q & -p & 0 \end{bmatrix} \tag{8}$$

After converting the variables $\widehat{x}_k$, z_k, and A, which have the form of the Kalman filter's system model, parameters $\widehat{x}_0$ P_0, Q, H, and R used in the algorithm are predetermined to complete the design of the Kalman filter algorithm. In the Kalman filter algorithm, four calculation steps are performed based on the determined variables and parameters to calculate the final attitude angle, which is a fusion of acceleration and gyroscopic signals. In the first Kalman filtering step, the predicted estimates $\widehat{x}_k^-$ and predicted error covariance P_k^- are determined:

$$\widehat{x}_k^- = A\widehat{x}_{k-1} \tag{9}$$

$$P_k^- = AP_{k-1}A^T + Q \tag{10}$$

where "−" represents a predicted state, A is identical to that in Eq. (9), and Q is a matrix determined by a designer before building the Kalman filter algorithm. In the second step, the Kalman gain K_k is calculated; it is the weight given to the P_k^-−based calculation of estimates in the previous step:

$$K_k = P_k^- H^T \left(HP_k^- H^T + R\right)^{-1} \tag{11}$$

where H and R are both matrices that are determined before implementing the Kalman filter algorithm. In the third step, $\widehat{x}_k$ is computed with z_k and K_k:

$$\widehat{x}_k = \widehat{x}_k^- + K_k\left(z_k - H\widehat{x}_k^-\right) \tag{12}$$

In the last step, P_k is calculated with the values obtained in the previous steps:

$$P_k = P_k^- - K_k H P_k^- \tag{13}$$

$\widehat{x}_k$ and P_k are updated and become $\widehat{x}_{k-1}$ and P_{k-1} in Eqs. (9) and (10) of the first step, respectively. We referred to Zhang and Liao [58] to set the parameters: $\widehat{x}_0 = [1 \quad 0 \quad 0 \quad 0]$, $P_0 = \mathrm{I}$, $Q = 0.01 \times \mathrm{I}$, $H = \mathrm{I}$, and $R = 0.01 \times \mathrm{I}$, where I represents a unit matrix. The calculated estimates $\widehat{x}_k = [q_1 \quad q_2 \quad q_3 \quad q_4]^T$ are converted into the final attitude angle ($x_{Attitude} = [\mathrm{phi} \quad \mathrm{theta} \quad \mathrm{psi}]^T$) with Eqs. (14)–(16):

$$\mathrm{phi} = \mathrm{atan2}\left(2q_3q_4 + q_1q_2, 1 - 2\left(q_2^2q_3^2\right)\right), \tag{14}$$

$$\mathrm{theta} = -\mathrm{asin}(2(q_2q_4 - q_1q_3)) \tag{15}$$

$$\mathrm{psi} = \mathrm{atan2}\left(2q_2q_3 + q_1q_4, 1 - 2\left(q_3^2q_4^2\right)\right) \tag{16}$$

The estimated final attitude angle $x_{Attitude}$ is expressed as the tilt Z:

$$Z = \begin{bmatrix} Z_x \\ Z_y \\ Z_z \end{bmatrix} = \begin{bmatrix} sin(\mathrm{theta}) \\ -cos(\mathrm{theta})sin(\mathrm{phi}) \\ -cos(\mathrm{theta})cos(\mathrm{phi}) \end{bmatrix} \tag{17}$$

To derive the external acceleration a^s from a sensor-based frame of reference, Z is multiplied by the gravitational acceleration g and then subtracted from each signal: $x_{acc} = [f_x \quad f_y \quad f_z]^T$ Lee [57]; this results in $a^s = \begin{bmatrix} a_x^s \\ a_y^s \\ a_z^s \end{bmatrix} = \begin{bmatrix} f_x - gZ_x \\ f_y - gZ_y \\ f_z - gZ_z \end{bmatrix}$. When the transpose of a^s is multiplied by Z, the vertical acceleration $a_z = (a^s)^T Z$ can be estimated from an inertial frame of reference.

When fused with the barometer's atmospheric pressure signal through the complementary filter, a_z can be used for the estimation of the vertical position. The complementary filter can be applied to signals that are mutually complementary; it is widely used to calibrate the altitude obtained from vertical acceleration signals based on the atmospheric pressure [59]. The atmospheric pressure P can be converted into the vertical displacement h based on the atmospheric pressure at sea level:

$$S_B = h = 44330\left(1 - \left(\frac{P}{P_0}\right)^{0.19}\right) \tag{18}$$

the unit of h is m, and P_0 is the atmospheric pressure at sea level (101,325 Pa). The fusion of h and the previously estimated a_z through the complementary filter results in the calculation of the vertical velocity v_z and vertical position h_z. When the state vector derived through the complementary filter is defined as $x_2 = [h_z \quad v_z]^T$, the complementary filter can be represented as follows [57]:

$$x_{2,t} = \begin{bmatrix} 1 & \Delta t \\ 0 & 1 \end{bmatrix} x_{2,t-1} + \begin{bmatrix} 1 & \Delta t/2 \\ 0 & 1 \end{bmatrix} \mathrm{K}_c \Delta t \times \varepsilon_{h,t-1} + \begin{bmatrix} \Delta t/2 \\ 1 \end{bmatrix} \Delta v_{z,t-1} \tag{19}$$

where ε_h is the difference between S_B calculated from the atmospheric pressure at sea level and h_z, which is the estimated vertical position and can be written as follows: $\varepsilon_{h,\,t-1} = S_{B,\,t-1} - h_{z,\,t-1}$ [57]. The change in the velocity over time is $\Delta v_z = \Delta t \times a_z$. The complementary filter gain of K_c is $\begin{bmatrix} \sqrt{2(\sigma_{acc}/\sigma_B)} \\ \sigma_{acc}/\sigma_B \end{bmatrix}$, and σ_{acc} and σ_B are the standard deviations of a_z and S_B, respectively.

The h_z values estimated from the base and belt modules were used to identify workers at height through rule-based analysis. Any difference in the estimated vertical position of each module that exceeded the threshold was classified as "work at height". It is defined as work performed at more than six feet (1.83m) by the OSHA [13]and at more than 2 m by the KOSHA [51]. This analysis is based on the KOSHA standard. Since the belt module was attached to the back of a worker's safety belt (i.e., a person's back), it was above the ground on which the workers stepped on. Therefore, the height of the sensors attached to the back was considered the height of the back of a typical safety belt: above 70% of 1.65 m, which is the average height of Koreans according to the Korean Statistical Information Service [60]. Thus, 1.2 m were added to the KOSHA's standard for work at height; the final threshold was 3.2 m.

2.4. Detection of fastening state of safety hook

The acceleration signals obtained from the belt and hook modules were used to detect fastening state of safety hooks. In this study, the velocity and displacement data, which can be obtained by integrating the acceleration data, were combined with acceleration signals, and the data were labeled according to the state of the safety hooks determined by the sequence of tasks of each subject. From the velocity and displacement data, the features were extracted according to the window size. The moving window with 25% shift (i.e., 75% overlap), which means if the window size is 100 seconds, the neighboring window shares 75 seconds of signals, is applied to extract the features. In total, 66 features were extracted, which represent the maximum, minimum, mean, standard deviation, sum, and cross-correlation of the velocity and displacement data for the x-, y-, and z-axes of each sensor.

The extracted features were used to train the representative machine learning algorithms to develop models for the detection of the fastening state of safety hooks; subsequently, the best-performing model was selected. Single and ensemble algorithm classifiers were chosen, which were used in previous studies for the classification of the activities of workers through IMU sensors [61,13,43]. For the single algorithm classifiers, decision trees [30], k-nearest neighbors (KNNs) [62,43], and support vector machines (SVMs) with the radial basis function (rbf) kernel (Gaussian rbf SVM) [63] were trained. For the ensemble algorithm classifier models, random forests (RFs; bagging on decision trees) [64,65] and the boosting algorithm of AdaBoost [43] were trained. All machine learning classifier models were subject to changes in the windows of up to 180 s (which is the duration of one section of the experiment) for comparative analysis of their accuracy. Through this process, we identified the window size with the best performance. The following section presents the trained classifier models.

Decision Tree (DT) takes advantage of training datasets to predict the labels of new datasets based on if-then-else decision rules [66]. In the decision tree algorithm, a tree represents decision making; it consists of a root node that constitutes all data, an internal node that represents attributes, and a leaf node that holds a class label [67.66]. Each node in the DT algorithm has only one parent node and two or more descendant nodes [67]. In the training stage, training datasets are grouped depending on their homogeneity; they branch out into either internal nodes or leaf nodes, whereas the root becomes the rules [66]. This process iterates until all leaf nodes form a tree. The test datasets follow the tree rules by which they are trained and identify leaf nodes to assign class labels [68]. DT makes no assumption about data distribution and is a strictly non-parametric algorithm [67] that ensures tree-based data classification; thereby, it simplifies visualization, understanding, and interpretation [66].

k-Nearest Neighbors (KNNs) is one of the non-parametric learning methods for regression and classification [66]. Such as DT, KNN makes no assumption about data distribution and is thus nonparametric. In KNN, k is the number of nearest neighbors, and the data labels for new data points are predicted by finding k nearby data points with similar features. In this process, the labels for the k nearest data points are determined by measuring the distances between new and trained data points. Finally, KNN casts a majority vote for adjacent labels and assigns the most voted label to new data. KNN is simple and intuitive because it makes no assumptions about the data in the training stage [66]. However, it has some limitations; it is sensitive to the magnitudes of datasets and outliers since it is based on the distance of data points when selecting neighbors.

Support Vector Machine (SVM) with rbf kernel (Gaussian rbf SVM) is one of the machine learning algorithms that can adjust the datasets of workers' body movements to the designated label for relevant classification. As an algorithm, SVM creates a non-probabilistic binary linear classifier that assigns classes to new data when a dataset that belongs to a certain class is available [69]. It assigns data classes based on the maximum-margin hyperplane that maximizes the margin (i.e., the distance between the hyperplane and nearest data point) for the training data mapped in space [70]. When new datasets are available, the algorithm assigns new data to classes that are closest to each margin. With SVM, it is challenging to address real-world classification problems in a simple hyperplane owing to their high level of complexity [70]. Through the use of kernel functions (e.g., Gaussian RBF, polynomial functions, etc.), it is possible to classify complex problems with nonlinear mapping in high-dimensional space [71,70]. In this study, we trained the SVM model by using the Gaussian radial basis function (RBF) kernel [72], which is the most widely used among various kernel functions.

Random Forest (RF) is an ensemble learning method that employs bagging to combine multiple decision trees with the decision tree algorithm as a base learner [73,45]. The method uses bootstrapping from training datasets to draw bootstrap samples for classification and regression [74,73]. For each bootstrap sample, a regression or classification tree is developed to select the best split for the predictors at each node. The RF method uses all random prediction results of the sample tree and forecasts the class labels for new datasets [75,73]. Furthermore, this method induces diversity between trees and maintains the prediction strength by selecting the best split among random subsets at each node [76]. Random predictor selection reduces the correlation among the trees and mitigates bias; in addition, it can reduce variance through the ensemble of unpruned trees [76,73]. Because RF can assess variable importance, the results can be used to compare the relative weights of predictors [76].

AdaBoost is an iterative algorithm that enhances the performance of combined classifiers by boosting any learning algorithm [77]. The core idea of AdaBoost is to train different weak classifiers with the same training sets and to combine these weak classifiers to turn them into stronger final ones [78]. The AdaBoost algorithm changes the data distribution based on the accuracy of a sample's correct classification and prior overall classification in each training set and determines the weight of each sample. New datasets with modified weights are trained in lower classifiers, which in turn undergo the fusion process to become stronger final ones [78]. The AdaBoost algorithm can improve prediction accuracy by enhancing the functions of weak classifiers while reducing bias and variance through continuous training to strengthen its data classification ability [78,79].

Before evaluating each model's performance, a randomized search algorithm was used for the hyperparameter tuning of each model. Since the performance of the machine learning models depends on the set hyperparameters, optimal hyperparameters must be chosen [80,45]. Grid search and randomized search are typical methods used for hyperparameter tuning [81]. Whereas grid search computes all combinations of parameters within the set range, randomized search computes randomly selected combinations within the set range; thus, it is time efficient. To test the performance of the hyperparameter combinations obtained through randomized search, the datasets were classified into training and testing sets (in a ratio of 8:2): 20% of the data were not used in the training processes; they were used exclusively to test the models. The models were trained with the frequently used 10-fold cross-validation method [82,81], where k is divided into 10 folds. The previously reserved testing set was used to evaluate the trained models. This testing process yielded the final combination of hyperparameters with the highest accuracy for the proposed models. This testing process yielded the final combination of hyperparameters with the highest accuracy for the models as summarized in Table 2.

In the DT algorithm, hyperparameters (e.g., the maximum depth, maximum number of branching leaf nodes, and classification criteria of nodes) can affect the DT performance [83]. Thus, we tried to adjust these hyperparameters to identify a valid DT model. Because k, which represents the nearest neighbors, is the most critical hyperparameter, the number of neighbors was adjusted [45]. The functions that compute weights assigned to nearest neighbors as well as the hyperparameters used to compute nearest neighbors were also adjusted because of their potential impact on the model performance [45]. The predictive performance of the SVM algorithm is affected by hyperparameters such as the kernel function, width (gamma), and regularization parameter (C) [84]. We employed the widely used rbf kernel and adjusted C representing the size of gamma (which is used to calibrate the impact between specific training data and the separation line) and margin [85]; in addition, we determined how much misclassification can be accepted. The RF method (a DT-based algorithm) can build an effective model with hyperparameters that represent the quality of splits and split processes [45]. The number of base learners must be prioritized when using the bagging method [45]. In the RF model, the tree's maximum depth was adjusted like the hyperparameters in DT. To build an effective RF model, the hyperparameters representing the quality of splits, split processes, and number of trees were further calibrated. Because the AdaBoost algorithm is also a DT-based ensemble method, the number of estimators can be a critical hyperparameter for the model performance

Table 2
List of hyperparameters used in randomized search.

Classifier	Hyperparameters	Range of values
Decision Tree	Maximum depth	{10–100} (Increase by 1) (**48**)
	Maximum number of branching leaf nodes	{5–100} (Increase by 5) (**100**)
	Classification criteria for nodes	{**entropy algorithm**, gini algorithm}
k-Nearest Neighbors	Number of neighbors	{10–~20}(Increase by 1) (**2**)
	Weight function	{uniform algorithm, **distance algorithm**}
	Algorithm used to compute the nearest neighbors	{auto algorithm, ball_tree algorithm, kd_tree algorithm, **brute algorithm**}
Gaussian RBF SVM	Kernel function	{**Gaussian RBF**, polynomial}
	Kernel width (gamma)	{0.01, 0.1, 1, 10, 100} (**0.001683375945728094**)
	Regularization parameter (C)	{0.01, 0.1, 1, 10, 100} (**4.627917891485669**)
Random Forest	Maximum depth of tree	{1–40} (Increase by 1) (**19**)
	Quality of splits	{**entropy algorithm**, gini algorithm}
	Split processes (min_samples_split)	{1–21} (Increase by 1) (**4**)
	Split processes (min_samples_leaf)	{1–21} (Increase by 1) (**3**)
	Number of trees	{10–500} (Increase by 10) (**280**)
AdaBoost	Number of trees	{10–1000} (Increase by 10) (**920**)
	Learning algorithm	{**SAMME**, SAMME.R algorithm}

(Bold: optimal value).

[86,45]; therefore, the number of trees was adjusted. The AdaBoost model was developed by using a learning algorithm that represents a boosting method as a hyperparameter. Stagewise additive modeling with a multi-class exponential loss function (SAMME) and SAMME.R algorithm, which utilizes real values of the probability of input samples belonging to different classes, have potential effect on the model performance [87,88]. Therefore, SAMME and SAMME. R algorithms, having been adjusted as hyperparameters, were used for model training.

Through the hyperparameter optimization of various algorithm models and the subsequent LOSOCV for the evaluation of the model performance, we selected the candidate model with the highest accuracy. Developing a model and evaluating its performance require the consideration of the individual characteristics of workers, such as the body movements, task performance, and individual variability [89]. Unlike k-fold cross-validation, LOSOCV, which treats one subject as a test set, trains models with the remaining subjects as training sets, computes their accuracy, and evaluates them based on the average of the accuracies derived from repeated testing on all subjects [90,33]. In this way, the LOSOCV method can be used to assess how precisely the developed model classifies data from new subjects that are not included in the training data, thus offering more realistic and accurate estimates in practice [91]. To monitor successfully new workers at a construction site, a model designed to detect the fastening state of safety hooks of workers at height must be able to make valid predictions for new subjects with different individual characteristics. By evaluating trained models with LOSOCV, this method intends to ensure generalizability such that the fastening state of safety hooks of new workers at height in different construction settings can be accurately monitored and detected.

3. Results

As described in Section 2.4, workers at height can be identified with the signals collected from the IMU and barometric sensors on the base and belt modules. The accuracy, precision, and recall of the rule-based model, which is used to identify workers at height, were assessed. A total of 43,200 data points were tested to identify workers at height; the developed model accurately classified 27,338 out of 28,800 datasets as “work at height”. From 14,400 datasets not considered “work at height”, the model accurately classified 14,187 datasets as “work at a lower level”. Fig. 4 shows that workers at height can be identified with high accuracy (96.1%). “Precision” is the index indicating the number of datasets of actual workers at height out of the datasets classified by the model as workers at height; “recall” is the index indicating the number of datasets identified by the model as “workers at height” out of the datasets of actual workers at height. The developed model has 99.3% precision and 94.9% recall; hence, it can accurately identify workers working at height in different construction environments.

As discussed in Section 2.5, a model was developed based on acceleration signals from the IMU sensor on the back and hook modules to detect the fastening state of safety hooks. Machine learning classifiers such as decision trees, KNNs, RFs, SVMs with rbf kernel, and AdaBoost were used to develop the model. The performance of the model identifying work at height was assessed in terms of accuracy, precision, and recall. Fig. 5 summarizes the results of the model accuracy evaluation (window sizes: 1–180 s) after hyperparameter tuning through 10-fold cross-validation and LOSOCV. The highest accuracy (86.0%; window size = 30 s) was achieved with the RF model, followed by AdaBoost (85.3%, window size = 20 s), decision tree (79.3%, window size = 40 s), SVM with rbf kernel (76.3%, window size = 4 s), and KNN (75.9%, window size = 20 s). Fig. 6 presents the precision and recall of the RF model depending on the window size; evidently, the values of precision and recall are reversed when the window is larger than 30 s. Because precision and recall have a trade-off relationship (i.e., one increases when the other decreases) [92], the results are best when the two strike a balance at a 30 s window.

In summary, the worker-at-height identification model is 96% accurate (as seen in Fig. 4), while the safety hook attachment detection model, which uses the RF algorithm, is 86% accurate for a 30 s window. All in all, the results of the safety monitoring system for workers at height are 83% accuracy, 86% precision, and 82% recall. In other words, the developed system can identify workers at height and detect the fastening state of safety hooks with 83% accuracy. In particular, the detection system can detect workers at height whose safety hooks are not fastened with 86.4% accuracy.

4. Discussion

4.1. Role of Kalman and complementary filters

We combined acceleration and gyroscopic signals from the IMU sensor with atmospheric pressure signals from the barometer to predict the altitudes of sensors with Kalman and complementary filters. Workers at height were identified based on the estimated altitude differences between the base and belt modules. The use of the Kalman and complementary filters yielded 96.12% accuracy; the accuracy without filtering method was 94.83%. The standard deviation of the accuracy by subject was 2.17% when the Kalman and complementary filters were used, which is approximately 1.6 times lower than when no filtering method was used (3.47%). Although the accuracy of identifying workers at height without filtering method is only approximately 2% lower than in the case with filtering method, the larger deviation causes the accuracy to decrease to 80% within the six-sigma range. When the Kalman and complementary filters were used, at least 90% accuracy was maintained within the six-sigma range. This is because the Kalman and complementary filters can aptly calibrate barometer signal errors that are caused by the body movements of workers with the IMU’s acceleration and gyroscopic signals. Hence, the filters enable the consistent and accurate identification of workers working in different construction environments at height (Fig. 7).

4.2. Feature importance of detection model for fastening state of safety hooks

The model converts acceleration signals from the hook and belt

Confusion Matrix		Actual (43,200ea)	
		T (Work at height)	F (Work at low height)
Predicted	T	27,338	213
	F	1,462	14,187

Accuracy : $\frac{27{,}338 + 14{,}187}{27{,}338 + 213 + 1{,}462 + 14{,}187} = \mathbf{0.961}$

Precision : $\frac{27{,}338}{27{,}338 + 213} = \mathbf{0.992}$

Recall : $\frac{27{,}338}{27{,}338 + 1{,}462} = \mathbf{0.949}$

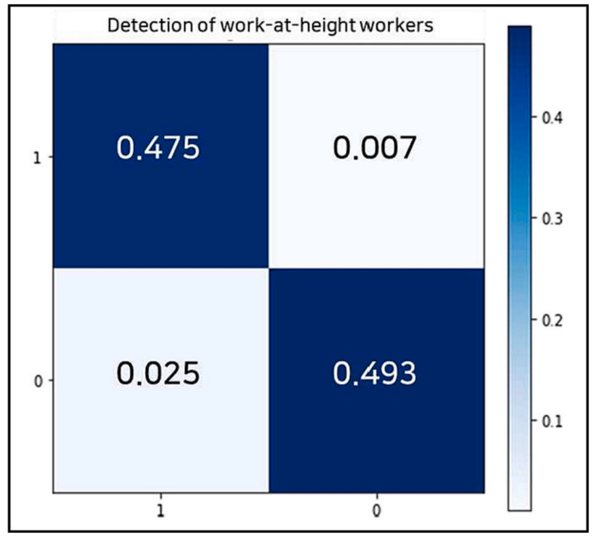

Fig. 4. Confusion matrix for detecting workers at height.

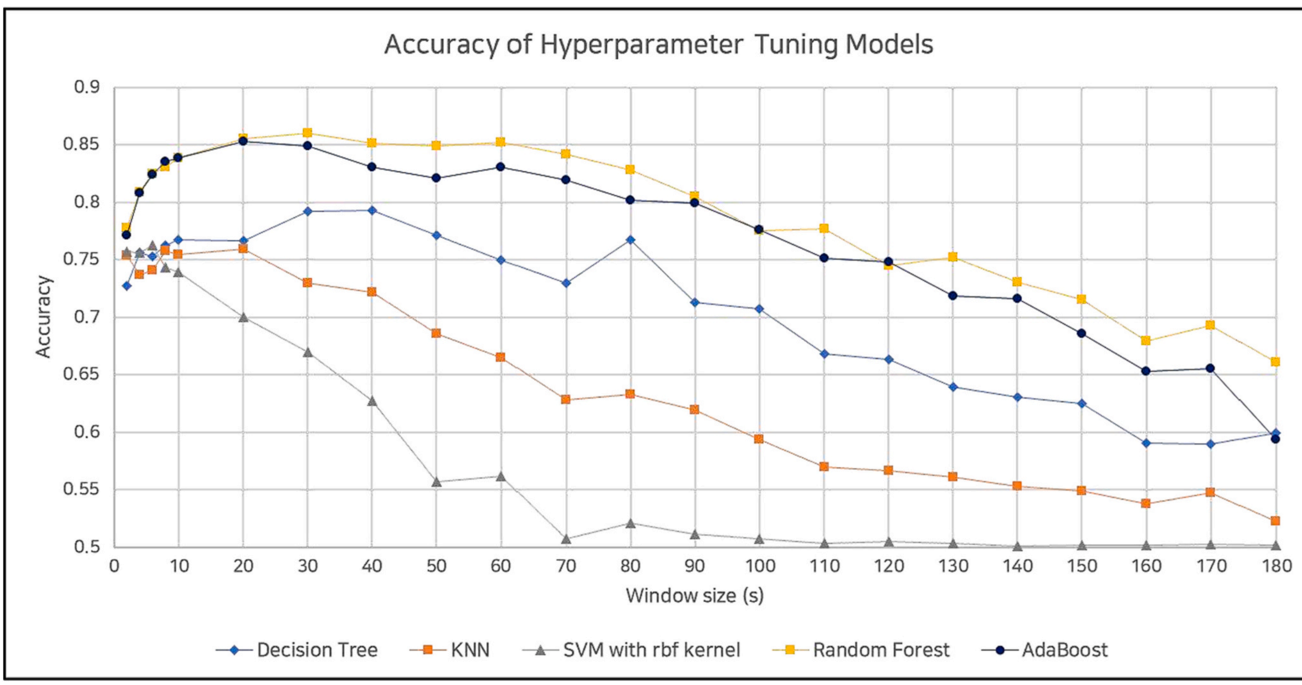

Fig. 5. Comparison of accuracy of classifier models.

modules into velocity and displacement data and extracts features depending on the size of the sliding window to train the RF algorithm. Selecting relevant features according to their importance can compress data and facilitate data processing, which is crucial for the development of future models [93]. Saving computation time and simplifying the process can be achieved with fewer resources [94]. We identified the features that played a pivotal role in the safety hook attachment detection model. The RF algorithm (window size = 30 s) with the highest accuracy was employed to determine the features of high significance. Fig. 8 shows the important features.

Evidently, the cross-correlation between the velocity and displacement of the safety belt and hook on the x- and y-axes (i.e., vx_corr, dx_corr, vy_corr, and dy_corr) all rank in the top ten out of 66 features. This indicates that the correlation between the safety hook and workers' front-to-back and side-to-side movements (x, y) is particularly important. When the safety hook of a worker at height at a construction site is securely attached to an anchor point, the safety hook does not move much, even when the worker moves a lot; this results in extremely low correlation. By contrast, improper attachment (e.g., when a worker attaches his/her safety hook to their own belt and not the anchor point) results in high correlation. Thus, the correlation between the safety belt and safety hook in terms of the workers' front-to-back and side-to-side movements (x- and y-axes) must be considered when developing a safety hook attachment detection model. Furthermore, out of the 22 features regarding front-to-back movements (x-axes), 16 features (approximately 73%) had a feature importance level higher than 0.01. This implies that the front-to-back movements of workers and their safety hooks were critical factors for the detection performance of the model. Twenty-five out of the 39 features with a feature importance level higher than 0.01 were safety hook-related; they confirm the importance of safety hook-related movements for the detection performance.

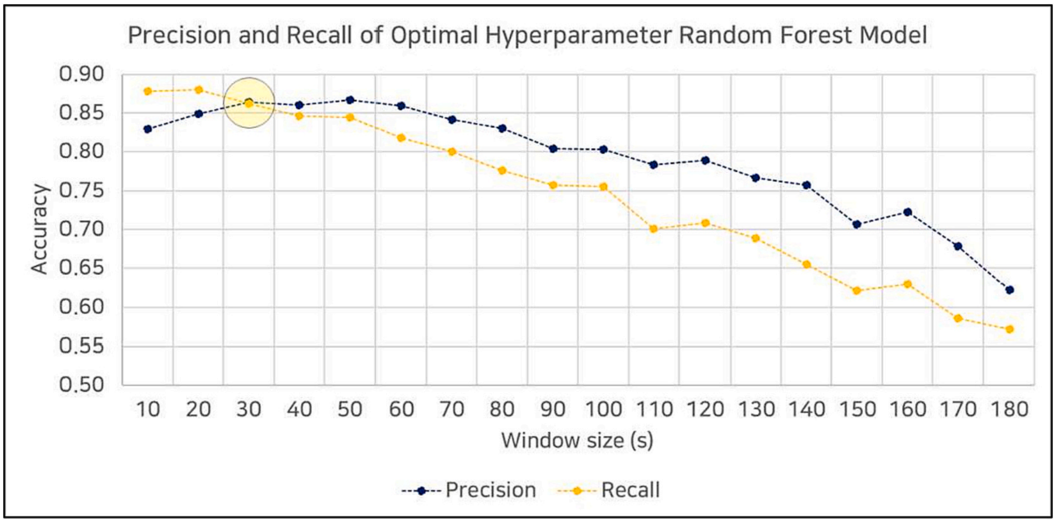

Fig. 6. Precision and recall of random forest (RF) model with optimal hyperparameter.

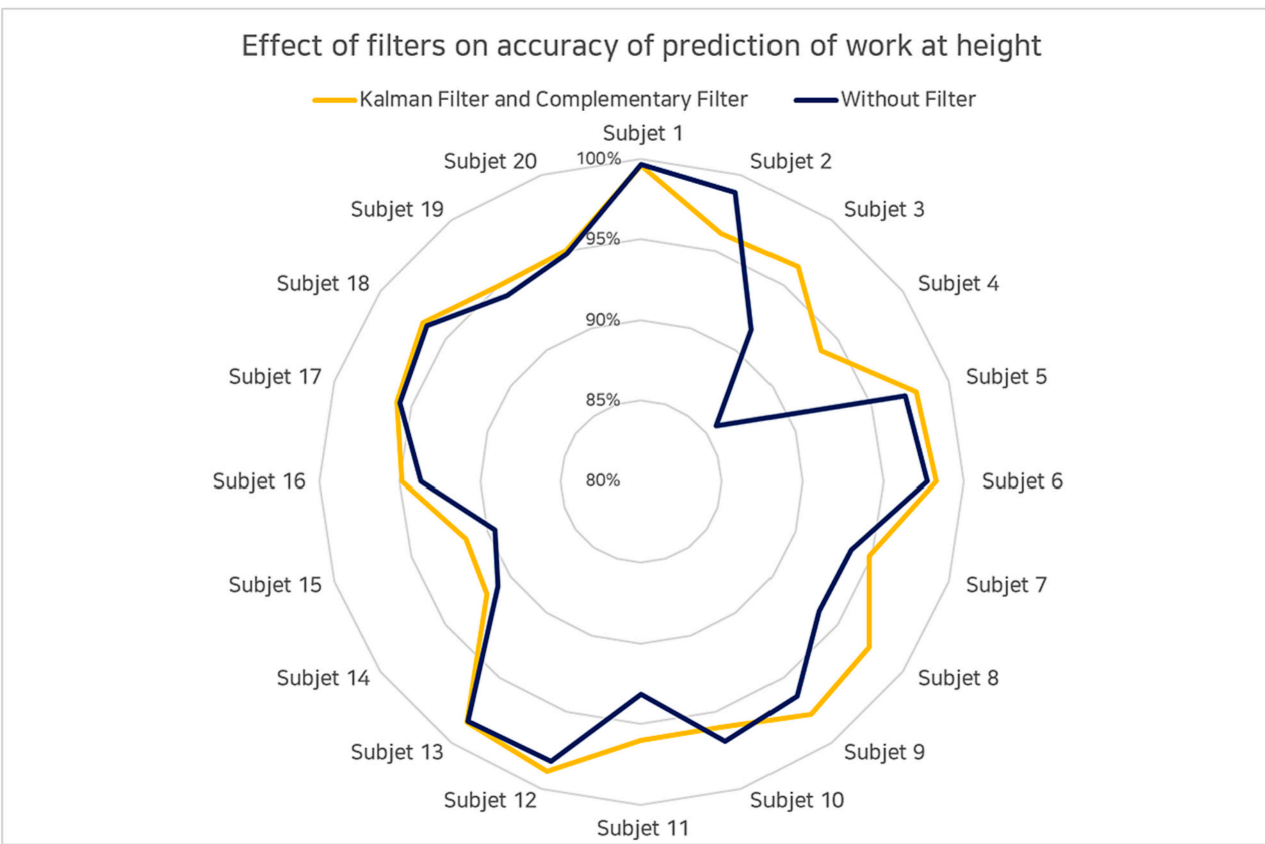

Fig. 7. Effect of filters on accuracy of identifying work at height.

The accuracy results of different types of features in the same RF machine learning model were comparatively analyzed. Fig. 9 compares the accuracy of the safety hook attachment detection model depending on the combinations of features. Accordingly, using only velocity features results in a higher accuracy than using only displacement features. Together with the previously presented analytical results, this finding confirms the significance of the correlation between the movements of the safety belt and safety hook. Fig. 8 also emphasizes the role of velocity features compared to that of displacement features. Because of the essential role of the correlation of velocity features, velocity-only training (rather than displacement-only training) resulted in higher model accuracy.

Wearing too many sensors can cause workers at actual construction sites to feel uncomfortable [95,96]. Using the minimum number of sensors can save money and time and is more practical at construction sites [43]. For example, when the number of modules (either one or two) has no effect on the performance of the model, using only one module is better. However, Fig. 10 shows that using only one module results in poorer performance than the model proposed in this study; thus, the safety belt and safety hook require two modules to assess the fastening

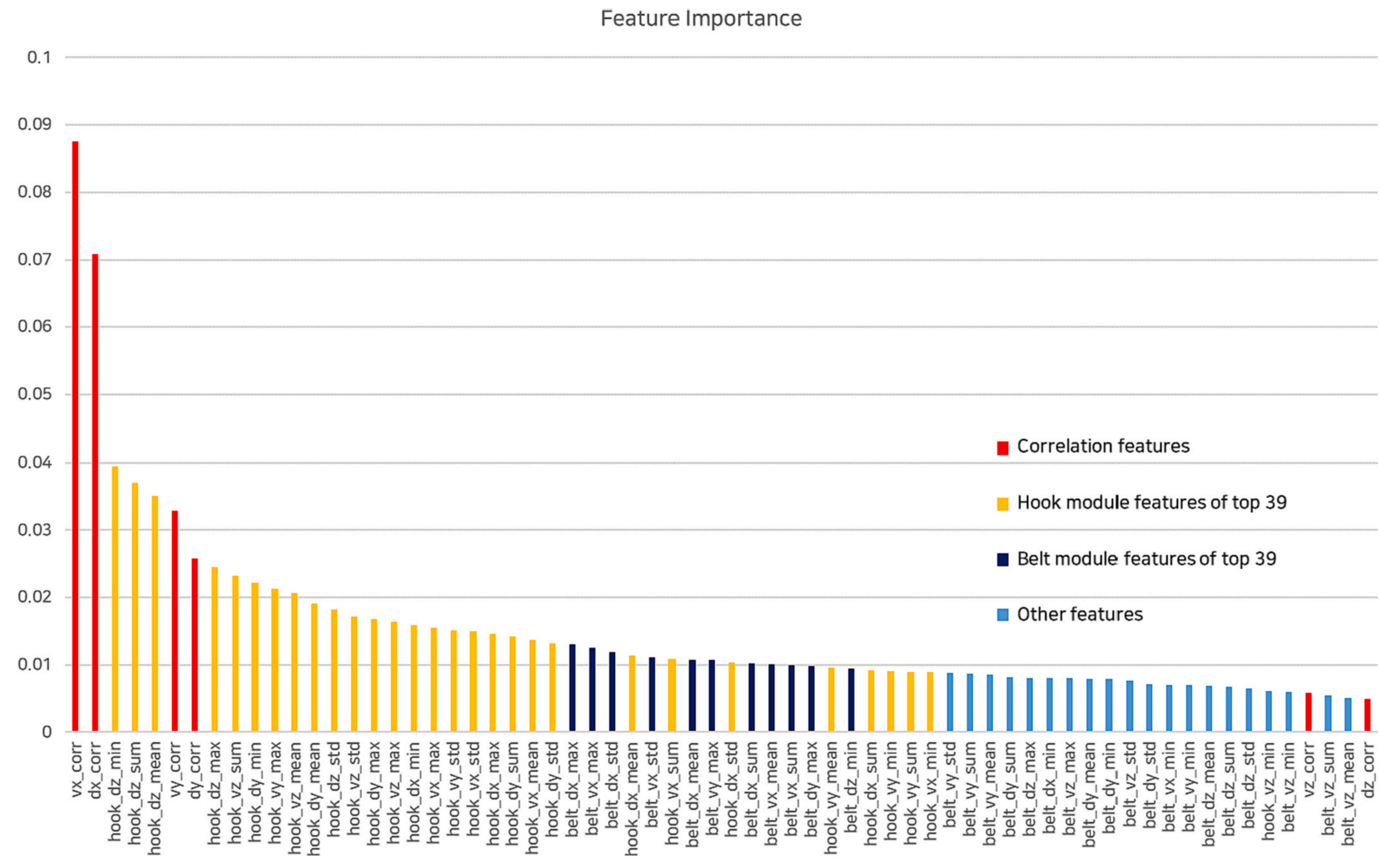

Fig. 8. Feature importance levels of RF models.

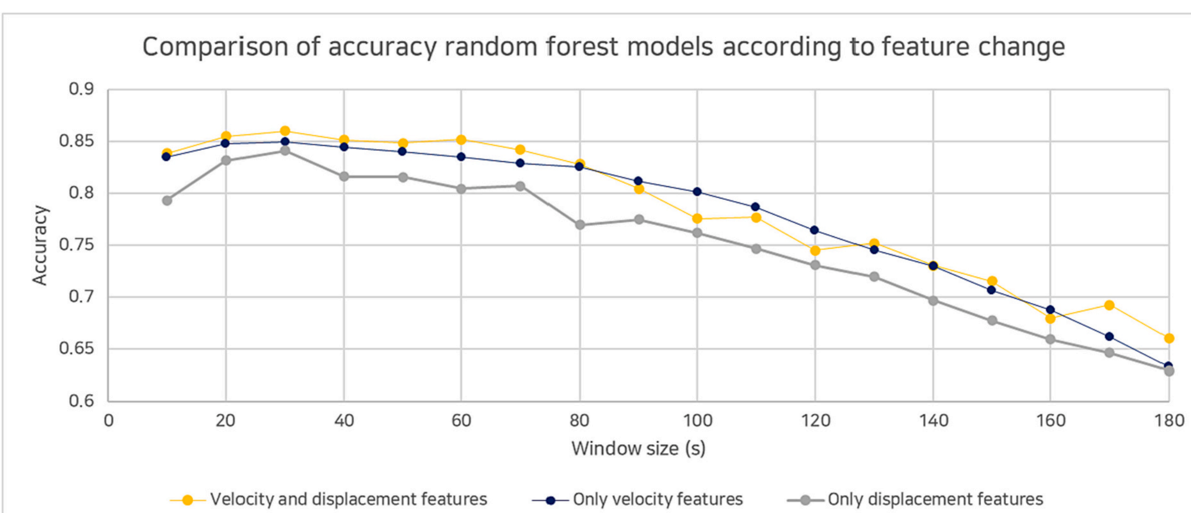

Fig. 9. Comparison of accuracy results of different features.

state of safety hooks of workers at height. Fig. 8 demonstrates that the correlation between the safety belt and safety hook cannot be emphasized enough; the use of both modules is indispensable. Furthermore, using only the safety hook module yielded higher accuracy than using only the safety belt module when detecting the fastening state of safety hooks. In Fig. 8, among the features that rank within the top 39, the features extracted from the hook module are more important than the ones extracted from the belt module. Thus, the hook module can be more helpful for detecting the fastening state of the safety hook because when the latter is securely attached, it rarely moves and when it is not attached, it moves much, such as the safety belt. This also implies that the movements of workers alone cannot help in the accurate detection of the fastening state of safety hooks.

4.3. Validation method

Ten-fold cross-validation, which is the most widely used method for the validation of machine learning classification, classifies data into ten folds. Nine folds are used for training, and the remaining fold is reserved for cross-validation, thereby increasing the possibility for the data of all

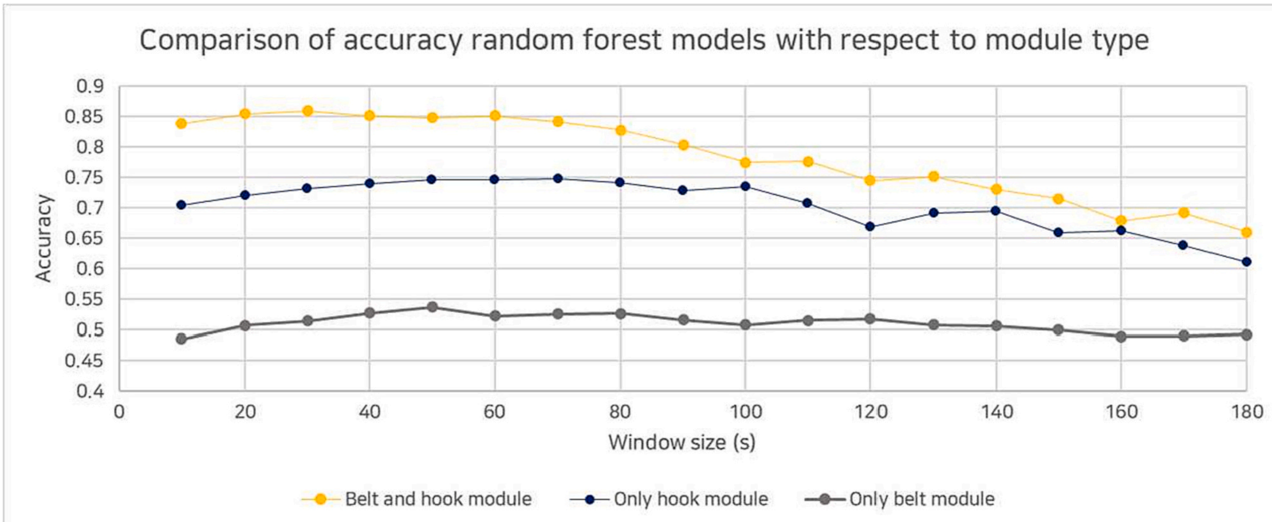

Fig. 10. Comparison of accuracy of RF models by module change.

subjects to be included in the training set [97]. Thus, the evaluation of models through k-fold cross-validation cannot ensure independence among subjects [89]. Because subject-specific body movements (e.g., the physical condition, motion, and posture) vary even for the same task [98,36], between-subject independence must be considered. By contrast, when LOSOCV is employed to evaluate the performance with one subject as a test set and the remaining subjects as training data, the accuracy of models for new subjects can be measured. This method considers variations in subject-specific characteristics when evaluating the performance of models and can, thus, assess the model's generalizability. We thoroughly reviewed previous studies [including those of Bangaru et al. [90], Lee et al. [33], Roberts et al. [99], and Wang et al. [100]] to check whether they confirm the validity of LOSOCV so that the models designed to classify the activities of construction workers can accept new subjects. Based on these considerations, LOSOCV was used for model evaluation (rather than the widely used k-fold cross-validation method) to determine the validity of the models developed to monitor and detect the fastening states of safety hooks of newly added construction workers during different tasks. Fig. 11 compares the evaluation method with k-fold cross-validation and the LOSOCV method used in this study. Evidently, the evaluation method using 10-fold cross-validation reaches 100% accuracy as the window size increases, whereas the accuracy of LOSOCV gradually decreases after achieving the highest accuracy. Thus, the safety hook attachment detection model developed in this study could have overfitted and overestimated the results if it had been combined with 10-fold cross-validation. The performance of the detection model with LOSOCV does not exhibit overfitting and overestimation for the fastening states of safety hooks of a wide array of workers.

To reiterate, the model proposed in this study can detect workers at height whose safety hooks are not fastened with 86.4% accuracy, which is comparable to the results obtained in previous studies (Khan et al. [102]: 99.8%, Lee et al. [103]: 96.58%, Song et al. [101]: 90.64%) on detecting the status of safety hooks. Considering that the results in this study were obtained using LOSOCV, the generalizability of the model in terms of adding new subjects is validated, and the level of accuracy achieved demonstrates the model's advancement.

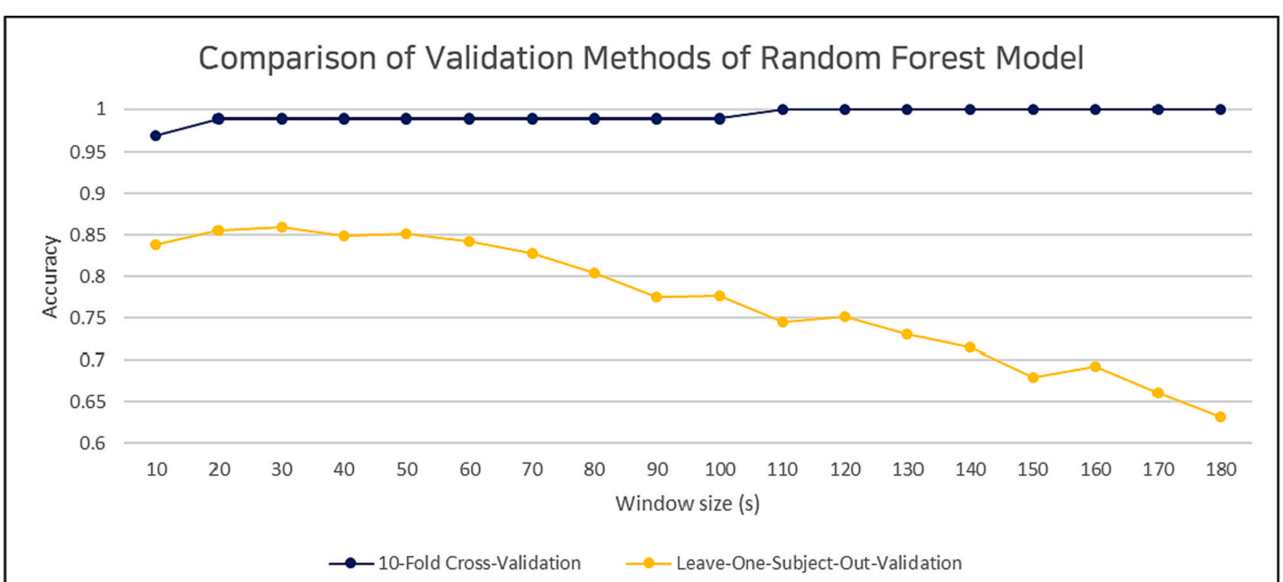

Fig. 11. Comparison between leave-one-subject-out cross-validation (LOSOCV) and 10-fold cross-validation methods.

4.4. Limitations and future works

We conducted a series of experiments under different working conditions by using mobile scaffolds and ladders for work at height and horse scaffolds and ground level work for work at a lower level. At actual construction sites, other types of work at height are performed, including work on mobile elevated work platforms and high-rise steel construction. In addition, we did not cover the case in which the safety hook is not attached to any point, for example, when it is lying on the floor, because such a case rarely occurs at construction sites. Therefore, more elaborate designs are required to extend the system's applicability for identifying a wider range of construction tasks in different construction environments. Regarding the field experiments at the construction site, the employed non-construction workers do not have enough experience regarding work at height. To generalize the model, further research is required to compile datasets from construction workers who have more experience. Last, the optimal window size of 30 s results in a 7.5 s time delay between the fastening state of the safety hook and model output. Considering that a worker at a site usually maintains a specific task for at least a few minutes [109], the time delay may not be a critical issue in monitoring the fastening state of the safety hook. However, further study, such as moving the window with a 1s shift, is required to detect unfastening or improper fastening of the safety hook immediately. Nonetheless, the results of the safety hook attachment detection system and its framework can prevent safety accidents, in particular, FFH. We believe that our detection system will be useful for the existing body of knowledge on FFH prevention in the construction industry.

5. Conclusion

We developed a safety monitoring system with IMU and barometer sensors to identify workers at height and the fastening state of safety hooks at complex and dynamic construction sites in real time. To verify the applicability of the developed safety monitoring system for practical use at construction sites, field experiments were conducted under different working conditions. Workers working at height were identified based on the atmospheric pressure and acceleration and gyroscopic signals from the IMU and barometer sensors that were attached to the workers. The fastening states of the safety hooks were determined with acceleration signals from the IMU sensor. The system with the rule-based approach identified workers at height with 96% accuracy. According to the performance evaluation of the safety hook attachment detection model (RF hyperparameter tuning) with LOSOCV, the model accuracy reached 86%. Thus, the performance of the model can be evaluated for new subjects, and the model can be used for different workers under different working conditions. Finally, the accuracy of the safety monitoring system (which combines the worker-at-height identification system with the safety hook attachment detection system) was 83%, which is high enough for efficient use in practice. This system enables on-site safety supervisors to monitor and detect improper fastening or unfastening actions of safety hooks by workers at height and to take necessary precautions to prevent FFH fatalities.

Declaration of Competing Interest

Byungjoo Choi reports financial support was provided by National Research Foundation of Korea.

Data availability

I have shared the link to the data in the manuscript.

Acknowledgement

This work was supported by the National Research Foundation of Korea (NFR) grant founded by the Korea Government (MSTI) (No.2020R1G1A1004797). The authors wish to thank their industry partners for their help in data collection, as well as anonymous participants who participated in the data collection.

References

[1] B. Choi, S. Lee, The psychological mechanism of construction workers' safety participation: The social identity theory perspective, J. Saf. Res. 82 (2022) 194–206, https://doi.org/10.1016/j.jsr.2022.05.011.

[2] B. Choi, S. Ahn, S. Lee, Construction workers' group norms and personal standards regarding safety behavior: Social identity theory perspective, J. Manag. Eng. 33 (4) (2017) 04017001, https://doi.org/10.1061/(ASCE)ME.1943-5479.0000511.

[3] B. Choi, H. Jebelli, S. Lee, Feasibility analysis of electrodermal activity (EDA) acquired from wearable sensors to assess construction workers' perceived risk, Saf. Sci. 115 (2019) (2019) 110–120, https://doi.org/10.1016/j.ssci.2019.01.022.

[4] J. Seo, S. Han, S. Lee, H. Kim, Computer vision techniques for construction safety and health monitoring, Adv. Eng. Inform. 29 (2) (2015) 239–251, https://doi.org/10.1016/j.aei.2015.02.001.

[5] U.S. Bureau of Labor Statistics (BLS), Table a-1. Fatal Occupational Injuries by Industry and Event or Exposure, All United States, 2020. https://www.bls.gov/iif/oshwc/cfoi/cftb0340.htm, 2021 (Accessed: Mar. 12, 2022).

[6] U.S. Bureau of Labor Statistics (BLS), Fatal and Nonfatal Falls, Slips, and Trips in the Construction Industry, 2020. www.bls.gov/opub/ted/2021/fatal-and-nonfatal-falls-slips-and-trips-in-the-construction-719, 2021 (Accessed: Mar. 12, 2022).

[7] W. Umer, H. Li, W. Lu, G.P.Y. Szeto, A.Y. Wong, Development of a tool to monitor static balance of construction workers for proactive fall safety management, Autom. Constr. 94 (2018) 438–448, https://doi.org/10.1016/j.autcon.2018.07.024.

[8] K. Yang, C.R. Ahn, M.C. Vuran, H. Kim, Collective sensing of workers' gait patterns to identify fall hazards in construction, Autom. Constr. 82 (2017) 166–178, https://doi.org/10.1016/j.autcon.2017.04.010.

[9] T.S. Abdelhamid, J.G. Everett, Identifying root causes of construction accidents, J. Constr. Eng. Manag. 126 (1) (2000) 52–60, https://doi.org/10.1061/(ASCE)0733-9364(2000)126:1(52).

[10] Y. Khosravi, H. Asilian-Mahabadi, E. Hajizadeh, N. Hassanzadeh-Rangi, H. Bastani, A.H. Behzadan, Factors influencing unsafe behaviors and accidents on construction sites: A review, Int. J. Occup. Saf. Ergon. 20 (1) (2014) 111–125, https://doi.org/10.1080/10803548.2014.11077023.

[11] M. Shin, H.-S. Lee, M. Park, M. Moon, S. Han, A system dynamics approach for modeling construction workers' safety attitudes behaviors, Accid. Anal. Prev. 68 (2014) 95–105, https://doi.org/10.1016/j.aap.2013.09.019.

[12] J. Reason, Human error, Camb. Univ. Press (1990), https://doi.org/10.1017/CBO9781139062367.

[13] M. Khan, R. Khalid, S. Anjum, N. Khan, S. Cho, C. Park, Tag and IoT based safety hook monitoring for prevention of falls from height, Autom. Constr. 136 (2022), 104153, https://doi.org/10.1016/j.autcon.2022.104153.

[14] M. Loosemore, N. Malouf, Safety training and positive safety attitude formation in the australian construction industry, Saf. Sci. 113 (2019) 233–243, https://doi.org/10.1016/j.ssci.2018.11.029.

[15] K. Yang, C.R. Ahn, M.C. Vuran, S.S. Aria, Semi-supervised near miss fall detection for ironworkers with a wearable inertial measurement unit, Autom. Constr. 68 (2016) 194–202, https://doi.org/10.1016/j.autcon.2016.04.007.

[16] T.K.M. Wong, S.S. Man, A.H.S. Chan, Critical factors for the use or non-use of personal protective equipment amongst construction workers, Saf. Sci. 126 (2020), 104663, https://doi.org/10.1016/j.ssci.2020.104663.

[17] W. Fang, L. Ding, H. Luo, P.E. Love, Falls from heights: A computer vision-based approach for safety harness detection, Autom. Constr. 91 (2018) 53–61, https://doi.org/10.1016/j.autcon.2018.02.018.

[18] X.S. Dong, J.A. Largay, S.D. Choi, X. Wang, C.T. Cain, N. Romano, Fatal falls and PFAS use in the construction industry: Findings from the NIOSH FACE reports, Accid. Anal. Prev. 102 (2017) 136–143, https://doi.org/10.1016/j.aap.2017.02.028.

[19] C.-F. Chi, T.-C. Chang, H.-I. Ting, Accident patterns and prevention measures for fatal occupational falls in the construction industry, Appl. Ergon. 36 (4) (2005) 391–400, https://doi.org/10.1016/j.apergo.2004.09.011.

[20] J.M. Gomez-de Gabriel, J.A. Fernandez-Madrigal, A. Lopez-Arquillos, J.C. Rubio-Romero, Monitoring harness use in construction with BLE beacons, Measurement 131 (2019) 329–340, https://doi.org/10.1016/j.measurement.2018.07.093.

[21] M.-W. Park, N. Elsafty, Z. Zhu, Hardhat-wearing detection for enhancing on-site safety of construction workers, J. Constr. Eng. Manag. 141 (9) (2015) 04015024, https://doi.org/10.1061/(ASCE)CO.1943-7862.0000974.

[22] Y. Piao, W. Xu, T.-K. Wang, J.-H. Chen, Dynamic fall risk assessment framework for construction workers based on dynamic Bayesian network and computer vision, J. Constr. Eng. Manag. 147 (12) (2021) 04021171, https://doi.org/10.1061/(ASCE)CO.1943-7862.0002200.

[23] H. Li, X. Yang, M. Skitmore, F. Wang, P. Forsythe, Automated classification of construction site hazard zones by crowd-sourced integrated density maps, Autom. Constr. 81 (2017) 328–339, https://doi.org/10.1016/j.autcon.2017.04.007.

[24] M. Liu, L. Xu, P.-C. Liao, Character-based hazard warning mechanics: A network of networks approach, Adv. Eng. Inform. 47 (2021), 101240, https://doi.org/10.1016/j.aei.2020.101240.
[25] M. Niu, R.M. Leicht, S. Rowlinson, Developing safety climate indicators in a construction working environment, Pract. Period. Struct. Des. Constr. 22 (4) (2017) 04017019, https://doi.org/10.1061/(ASCE)SC.1943-5576.0000340.
[26] X. Xing, B. Zhong, H. Luo, T. Rose, J. Li, M.F. Antwi-Afari, Effects of physical fatigue on the induction of mental fatigue of construction workers: A pilot study based on a neurophysiological approach, Autom. Constr. 120 (2020), 103381, https://doi.org/10.1016/j.autcon.2020.103381.
[27] T. Cheng, J. Teizer, Real-time resource location data collection and visualization technology for construction safety and activity monitoring applications, Autom. Constr. 34 (2013) 3–15, https://doi.org/10.1016/j.autcon.2012.10.017.
[28] M.J. Skibniewski, Information technology applications in construction safety assurance, J. Civ. Eng. Manag. 20 (6) (2014) 778–794, https://doi.org/10.3846/13923730.2014.987693.
[29] M. Zhang, T. Cao, X. Zhao, Applying sensor-based technology to improve construction safety management, Sensors 17 (8) (2017) 1841, https://doi.org/10.3390/s17081841.
[30] M. Zhang, S. Chen, X. Zhao, Z. Yang, Research on construction workers' activity recognition based on smartphone, Sensors 18 (8) (2018) 2667, https://doi.org/10.3390/s18082667.
[31] C.R. Ahn, S. Lee, C. Sun, H. Jebelli, K. Yang, B. Choi, Wearable sensing technology applications in construction safety and health, J. Constr. Eng. Manag. 145 (11) (2019) 03119007, https://doi.org/10.1061/(ASCE)CO.1943-7862.0001708.
[32] L. Chen, J. Hoey, C.D. Nugent, D.J. Cook, Z. Yu, Sensor-based activity recognition, IEEE Trans. Syst. Man Cybern. Part C Appl. Rev. 42 (6) (2012) 790–808, https://doi.org/10.1109/TSMCC.2012.2198883.
[33] G. Lee, B. Choi, H. Jebelli, C.R. Ahn, S. Lee, Noise reference signal–based denoising method for EDA collected by multimodal biosensor wearable in the field, J. Comput. Civ. Eng. 34 (6) (2020) 04020044, https://doi.org/10.1061/(ASCE)CP.1943-5487.0000927.
[34] J. Kim, S. Chi, J. Seo, Interaction analysis for vision-based activity identification of earthmoving excavators and dump trucks, Autom. Constr. 87 (2018) 297–308, https://doi.org/10.1016/j.autcon.2017.12.016.
[35] D. Kim, M. Liu, S. Lee, V.R. Kamat, Remote proximity monitoring between mobile construction resources using camera-mounted UAVs, Autom. Constr. 99 (2019) 168–182, https://doi.org/10.1016/j.autcon.2018.12.014.
[36] X. Yan, H. Li, A.R. Li, H. Zhang, Wearable IMU-based real-time motion warning system for construction workers' musculoskeletal disorders prevention, Autom. Constr. 74 (2017) 2–11, https://doi.org/10.1016/j.autcon.2016.11.007.
[37] Y. Yu, H. Li, X. Yang, L. Kong, X. Luo, A.Y. Wong, An automatic and non-invasive physical fatigue assessment method for construction workers, Autom. Constr. 103 (2019) 1–12, https://doi.org/10.1016/j.autcon.2019.02.020.
[38] D. Liu, Z. Jin, J. Gambatese, Scenarios for integrating IPS–IMU system with BIM technology in construction safety control, Pract. Period. Struct. Des. Constr. 25 (1) (2020) 05019007, https://doi.org/10.1061/(ASCE)SC.1943-5576.0000465.
[39] H. Ye, K. Dong, T. Gu, Himeter: Telling you the height rather than the altitude, Sensors 18 (6) (2018) 1712, https://doi.org/10.3390/s18061712.
[40] J. Chen, C.R. Ahn, S. Han, Detecting the hazards of lifting and carrying in construction through a coupled 3D sensing and IMUs sensing system, in: 2014 International Conference on Computing in Civil Engineering, 2014, pp. 1110–1117, https://doi.org/10.1061/9780784413616.138.
[41] T. Cheng, G.C. Migliaccio, J. Teizer, U.C. Gatti, Data fusion of real-time location sensing and physiological status monitoring for ergonomics analysis of construction workers, J. Comput. Civ. Eng. 27 (3) (2013) 320–335, https://doi.org/10.1061/(ASCE)CP.1943-5487.0000222.
[42] H. Jebelli, C.R. Ahn, T.L. Stentz, Fall risk analysis of construction workers using inertial measurement units: Validating the usefulness of the postural stability metrics in construction, Saf. Sci. 84 (2016) 161–170, https://doi.org/10.1016/j.ssci.2015.12.012.
[43] L. Sanhudo, D. Calvetti, J.P. Martins, N.M. Ramos, P. Meda, M.C. Goncalves, H. Sousa, Activity classification using accelerometers and machine learning for complex construction worker activities, J. Build. Eng. 35 (2021), 102001, https://doi.org/10.1016/j.jobe.2020.102001.
[44] J. Park, K. Kim, Y.K. Cho, Framework of automated construction safety monitoring using cloud-enabled BIM and BLE mobile tracking sensors, J. Constr. Eng. Manag. 143 (2) (2017) 05016019, https://doi.org/10.1061/(ASCE)CO.1943-7862.0001223.
[45] L. Yang, A. Shami, On hyperparameter optimization of machine learning algorithms: Theory and practice, Neurocomputing 415 (2020) 295–316, https://doi.org/10.1016/j.neucom.2020.07.061.
[46] Z. Wang, Y. Wu, L. Yang, A. Thirunavukarasu, C. Evison, Y. Zhao, Fast personal protective equipment detection for real construction sites using deep learning approaches, Sensors 21 (10) (2021) 3478, https://doi.org/10.3390/s21103478.
[47] J. Wu, N. Cai, W. Chen, H. Wang, G. Wang, Automatic detection of hardhats worn by construction personnel: A deep learning approach and benchmark dataset, Autom. Constr. 106 (2019), 102894, https://doi.org/10.1016/j.autcon.2019.102894.
[48] R. Xiong, P. Tang, Pose guided anchoring for detecting proper use of personal protective equipment, Autom. Constr. 130 (2021), 103828, https://doi.org/10.1016/j.autcon.2021.103828.
[49] M. Khan, R. Khalid, S. Anjum, N. Khan, S. Cho, C. Park, Fall prevention from scaffolding using computer vision and IoT-based monitoring, J. Constr. Eng. Manag. 148 (7) (2022) 04022051, https://doi.org/10.1061/(ASCE)CO.1943-7862.0002278.
[50] Occupational Safety and Health Administration (OSHA), Duty to Have Fall Protection. https://www.osha.gov/lawsregs/regulations/standardnumber/1926/1926.501, 1995 (Accessed: Mar. 12, 2022).
[51] Korea Occupational Safety and Health Agency (KOSHA), Rules on Occupational Safety and Health Standards. https://www.law.go.kr/, 2021 (Accessed: Mar. 12, 2022).
[53] C. Leys, C. Ley, O. Klein, P. Bernard, L. Licata, Detecting outliers: Do not use standard deviation around the mean, use absolute deviation around the median, J. Exp. Soc. Psychol. 49 (4) (2013) 764–766, https://doi.org/10.1016/j.jesp.2013.03.013.
[54] S. Aroni, R.A. Marino, K.S. Girven, J.M. Irving, J.F. Cheer, D.R. Sparta, Repeated binge ethanol drinking enhances electrical activity of central amygdala corticotropin releasing factor neurons in vivo, Neuropharmacology 189 (2021), 108527, https://doi.org/10.1016/j.neuropharm.2021.108527.
[55] X. Zhao, S. Barber, C.C. Taylor, Z. Milan, Classification tree methods for panel data using wavelet-transformed time series, Comput. Stat. Data Anal. 127 (2018) 204–216, https://doi.org/10.1016/j.csda.2018.05.019.
[56] H.-G. Min, J.-H. Yoon, J.-H. Kim, S.-H. Kwon, E.-T. Jeung, Design of Complementary Filter using Least Square Method, J. Inst. Control Robot. Syst. 17 (20) (2011) 125–130, https://doi.org/10.5302/j.icros.2011.17.2.125.
[57] J.K. Lee, A two-step Kalman/complementary filter for estimation of vertical position using an IMU-barometer system, J. Sensor Sci. Technol. 25 (3) (2016) 202–207, https://doi.org/10.5369/JSST.2016.25.3.202.
[58] T. Zhang, Y. Liao, Attitude measure system based on extended Kalman filter for multi-rotors, Comput. Electron. Agric. 134 (2017) 19–26, https://doi.org/10.1016/j.compag.2016.12.021.
[59] S. Wei, G. Dan, H. Chen, Altitude data fusion utilising differential measurement and complementary filter, IET Sci. Meas. Technol. 10 (8) (2016) 874–879, https://doi.org/10.1049/iet-smt.2016.0118.
[60] Korea Statistical Information Service (KOSIS), Distribution of Average Height of Gender by Age by City and Province: General. https://kosis.kr/, 2021 (Accessed: Mar. 12, 2022).
[61] M.F. Antwi-Afari, H. Li, Fall risk assessment of construction workers based on biomechanical gait stability parameters using wearable insole pressure system, Adv. Eng. Inform. 38 (2018) 683–694, https://doi.org/10.1016/j.aei.2018.10.002.
[62] R. Akhavian, A.H. Behzadan, Smartphone-based construction workers' activity recognition and classification, Autom. Constr. 71 (2016) 198–209, https://doi.org/10.1016/j.autcon.2016.08.015.
[63] M.F. Antwi-Afari, H. Li, Y. Yu, L. Kong, Wearable insole pressure system for automated detection and classification of awkward working postures in construction workers, Autom. Constr. 96 (2018) 433–441, https://doi.org/10.1016/j.autcon.2018.10.004.
[64] M.F. Antwi-Afari, H. Li, J. Seo, A.Y.L. Wong, Automated detection and classification of construction workers' loss of balance events using wearable insole pressure sensors, Autom. Constr. 96 (2018) 189–199, https://doi.org/10.1016/j.autcon.2018.09.010.
[65] M.F. Antwi-Afari, H. Li, W. Umer, Y. Yu, X. Xing, Construction activity recognition and ergonomic risk assessment using a wearable insole pressure system, J. Constr. Eng. Manag. 146 (7) (2020) 04020077, https://doi.org/10.1061/(ASCE)CO.1943-7862.0001849.
[66] Y. Wang, Y. Zhang, Y. Lu, X. Yu, A comparative assessment of credit risk model based on machine learning——a case study of bank loan data, Proc. Comput. Sci 174 (2020) 141–149, https://doi.org/10.1016/j.procs.2020.06.069.
[67] M.A. Friedl, C.E. Brodley, Decision tree classification of land cover from remotely sensed data, Remote Sens. Environ. 61 (3) (1997) 399–409, https://doi.org/10.1016/S0034-4257(97)00049-7.
[68] D. Muhajir, M. Akbar, A. Bagaskara, R. Vinarti, Improving classification algorithm on education dataset using hyperparameter tuning, Proc. Comput. Sci 197 (2022) 538–544, https://doi.org/10.1016/j.procs.2021.12.171.
[69] A.D. Dolatabadi, S.E.Z. Khadem, B.M. Asl, Automated diagnosis of coronary artery disease (CAD) patients using optimized SVM, Comput. Methods Prog. Biomed. 138 (2017) 117–126, https://doi.org/10.1016/j.cmpb.2016.10.011.
[70] W. Wang, Z. Xu, W. Lu, X. Zhang, Determination of the spread parameter in the Gaussian kernel for classification and regression, Neurocomputing 55 (3-4) (2003) 643–663, https://doi.org/10.1016/S0925-2312(02)00632-X.
[71] S. Suthaharan, Support vector machine, in: Machine Learning Models and Algorithms for Big Data Classification. Integrated Series in Information Systems 36, Springer, Boston, MA, 2016, https://doi.org/10.1007/978-1-4899-7641-3_9.
[72] S.S. Keerthi, C.-J. Lin, Asymptotic behaviors of support vector machines with Gaussian kernel, Neural Comput. 15 (7) (2003) 1667–1689, https://doi.org/10.1162/089976603321891855.
[73] S. Shakerian, M. Habibnezhad, A. Ojha, G. Lee, Y. Liu, H. Jebelli, S. Lee, Assessing occupational risk of heat stress at construction: A worker-centric wearable sensor-based approach, Saf. Sci. 142 (2021), 105395, https://doi.org/10.1016/j.ssci.2021.105395.
[74] A. Liaw, M. Wiener, Classification and regression by randomforest, R News 2 (2002) 18–22. https://www.r-project.org/doc/Rnews/Rnews_2002-3.pdf.
[75] L. Breiman, Random forests, Mach. Learn. 45 (2001) 5–32, https://doi.org/10.1023/A:1010933404324.
[76] A.M. Prasad, L.R. Iverson, A. Liaw, Newer classification and regression tree techniques: bagging and random forests for ecological prediction, Ecosystems 9 (2006) 181–199, https://doi.org/10.1007/s10021-005-0054-1.
[77] Y. Freund, R.E. Schapire, Experiments with a new boosting algorithm, in: Proceedings of the Thirteenth International Conference on International Conference on Machine Learning, 1996, pp. 148–156 (ISBN: 978-1-55860-419-3).

[78] Y. Wu, Y. Ke, Z. Chen, S. Liang, H. Zhao, H. Hong, Application of alternating decision tree with adaboost and bagging ensembles for landslide susceptibility mapping, Catena 187 (2020), 104396, https://doi.org/10.1016/j.catena.2019.104396.
[79] C. Ying, M. Qi-Guang, L. Jia-Chen, G. Lin, Advance and prospects of adaboost algorithm, Acta Automat. Sin. 39 (6) (2013) 745–758, https://doi.org/10.1016/S1874-1029(13)60052-X.
[80] P. Schratz, J. Muenchow, E. Iturritxa, J. Richter, A. Brenning, Hyperparameter tuning and performance assessment of statistical and machine-learning algorithms using spatial data, Ecol. Model. 406 (2019) 109–120, https://doi.org/10.1016/j.ecolmodel.2019.06.002.
[81] L. Torre-Tojal, A. Bastarrika, A. Boyano, J.M. Lopez-Guede, Graña, M., Above-ground biomass estimation from lidar data using random forest algorithms, J. Comput. Sci. 58 (2022), 101517, https://doi.org/10.1016/j.jocs.2021.101517.
[82] V.A. Dev, M.R. Eden, Formation lithology classification using scalable gradient boosted decision trees, Comput. Chem. Eng. 128 (2019) 392–404, https://doi.org/10.1016/j.compchemeng.2019.06.001.
[83] K.-M. Osei-Bryson, Evaluation of decision trees: a multi-criteria approach, Comput. Oper. Res. 31 (11) (2004) 1933–1945, https://doi.org/10.1016/S0305-0548(03)00156-4.
[84] R.G. Mantovani, A.L. Rossi, E. Alcobaca, J. Vanschoren, A.C. de Carvalho, A meta-learning recommender system for hyperparameter tuning: Predicting when tuning improves SVM classifiers, Inf. Sci. 501 (2019) 193–221, https://doi.org/10.1016/j.ins.2019.06.005.
[85] G. Battineni, N. Chintalapudi, F. Amenta, Machine learning in medicine: Performance calculation of dementia prediction by support vector machines (SVM), Informa. Med. Unlocked 16 (2019), 100200, https://doi.org/10.1016/j.imu.2019.100200.
[86] E. Sevinc, An empowered adaboost algorithm implementation: A covid-19 dataset study, Comput. Ind. Eng. 165 (2022), 107912, https://doi.org/10.1016/j.cie.2021.107912.
[87] T. Hastie, S. Rosset, J. Zhu, H. Zou, Multi-class adaboost, Statistics and Its, Interface 2 (2009) 349–360, https://doi.org/10.4310/SII.2009.v2.n3.a8.
[88] A. Taherkhani, G. Cosma, T.M. McGinnity, Adaboost-CNN: An adaptive boosting algorithm for convolutional neural networks to classify multi-class imbalanced datasets using transfer learning, Neurocomputing 404 (2020) 351–366, https://doi.org/10.1016/j.neucom.2020.03.064.
[89] G. Lee, S. Lee, Importance of testing with independent subjects and contexts for machine-learning models to monitor construction workers' psychophysiological responses, J. Constr. Eng. Manag. 148 (9) (2022) 04022082, https://doi.org/10.1061/(ASCE)CO.1943-7862.0002341.
[90] S.S. Bangaru, C. Wang, S.A. Busam, F. Aghazadeh, ANN-based automated scaffold builder activity recognition through wearable EMG and IMU sensors, Autom. Constr. 126 (2021), 103653, https://doi.org/10.1016/j.autcon.2021.103653.
[91] D. Gholamiangonabadi, N. Kiselov, K. Grolinger, Deep neural networks for human activity recognition with wearable sensors: Leave one-subject-out cross validation for model selection, IEEE Access 8 (2020) 133982–133994, https://doi.org/10.1109/ACCESS.2020.3010715.
[92] M. Buckland, F. Gey, The relationship between recall and precision, J. Am. Soc. Inf. Sci. 45 (1) (1994) 12–19, https://doi.org/10.1002/(SICI)1097-4571(199401)45:1%3C12::AID-ASI2%3E3.0.CO;2-L.
[93] J. Cai, J. Luo, S. Wang, S. Yang, Feature selection in machine learning: A new perspective, Neurocomputing 300 (2018) 70–79, https://doi.org/10.1016/j.neucom.2017.11.077.
[94] G. Wei, J. Zhao, Y. Feng, A. He, J. Yu, A novel hybrid feature selection method based on dynamic feature importance, Appl. Soft Comput. 93 (2020), 106337, https://doi.org/10.1016/j.asoc.2020.106337.
[95] S. Chernbumroong, A.S. Atkins, H. Yu, Activity classification using a single wrist-worn accelerometer, in: Proceedings of the 5th International Conference on Software, Knowledge Information, Industrial Management and Applications (SKIMA), IEEE, 2011, pp. 1–6, https://doi.org/10.1109/SKIMA.2011.6089975.
[96] B. Choi, S. Hwang, S. Lee, What drives construction workers' acceptance of wearable technologies in the workplace?: Indoor localization and wearable health devices for occupational safety and health, Autom. Constr. 84 (2017) 31–41, https://doi.org/10.1016/j.autcon.2017.08.005.
[97] J.-H. Kim, Estimating classification error rate: Repeated cross validation, repeated hold-out and bootstrap, Comput. Stat. Data Anal. 53 (11) (2009) 3735–3745, https://doi.org/10.1016/j.csda.2009.04.009.
[98] E. Valero, A. Sivanathan, F. Bosche, M. Abdel-Wahab, Analysis of construction trade worker body motions using a wearable and wireless motion sensor network, Autom. Constr. 83 (2017) 48–55, https://doi.org/10.1016/j.autcon.2017.08.001.
[99] D. Roberts, W. Torres Calderon, S. Tang, M. Golparvar-Fard, Vision based construction worker activity analysis informed by body posture, J. Comput. Civ. Eng. 34 (4) (2020) 04020017, https://doi.org/10.1061/(ASCE)CP.1943-5487.0000898.
[100] M. Wang, Y. Zhao, P.-C. Liao, EEG-based work experience prediction using hazard recognition, Autom. Constr. 136 (2022), 104151, https://doi.org/10.1016/j.autcon.2022.104151.
[101] K.-S. Song, S. Kang, D.-G. Lee, Y.-H. Nho, J.-S. Seo, D.-S. Kwon, A motion similarity measurement method of two mobile devices for safety hook fastening state recognition, IEEE Access 10 (2022) 8804–8815, https://doi.org/10.1109/ACCESS.2022.3144144.
[102] M. Khan, R. Khalid, S. Anjum, N. Khan, C. Park, IMU based Smart safety hook for fall prevention at construction sites, in: Proceedings of the 2021 IEEE Region 10 Symposium (TENSYMP), 2021, pp. 1–6, https://doi.org/10.1109/TENSYMP52854.2021.9550944.
[103] H. Lee, N. Kim, C.R. Ahn, Detecting hook attachments of a safety harness using inertial measurement unit sensors, in: Proceedings of the 38th International Symposium on Automation and Robotics in Construction, 2021, pp. 583–589 (ISBN 978-952-69524-1-3).
[104] CPWR Statistics, CPWR "Fatal and Nonfatal Injuries in Construction". https://www.cpwr.com/research/data-center/data-dashboards/fatal-and-nonfatal-injuries-in-construction/ (accessed September 20, 2022).
[105] O. Golovina, J. Teizer, K.W. Johansen, M. König, Towards autonomous cloud-based close call data management for construction equipment safety, Autom. Constr. 132 (2021), 103962, https://doi.org/10.1016/j.autcon.2021.103962.
[106] X. Yang, Y. Yu, S. Shirowzhan, H. Li, Automated PPE-Tool pair check system for construction safety using smart IoT, J. Build. Eng. 32 (2020), 101721, https://doi.org/10.1016/j.jobe.2020.101721.
[107] J. Zhao, E. Obonyo, G. Bilén, S., Wearable inertial measurement unit sensing system for musculoskeletal disorders prevention in construction, Sensors 21 (4) (2021) 1324, https://doi.org/10.3390/s21041324.
[108] B. Choi, Automated detection of construction workers that work at height and fastening state of safety hooks with wearable sensors, Mendeley Data V1 (2022), https://doi.org/10.17632/bwdvdy96mb.1.
[109] G. Lee, B. Choi, H. Jebelli, S. Lee, Assessment of construction workers' perceived risk using physiological data from wearable sensors: A machine learning approach, J. Build. Eng. 42 (2021), 102824, https://doi.org/10.1016/j.jobe.2021.102824.